



Towards quantum information processing with spins in silicon

Thomas Schenkel

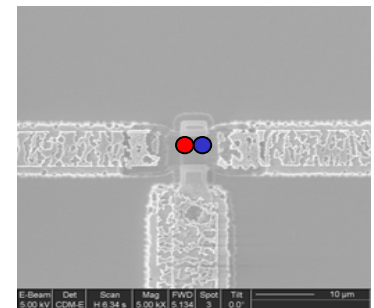
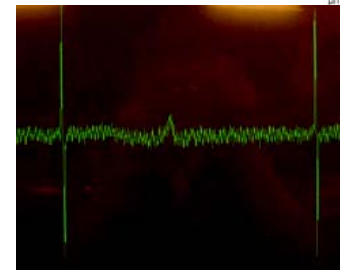
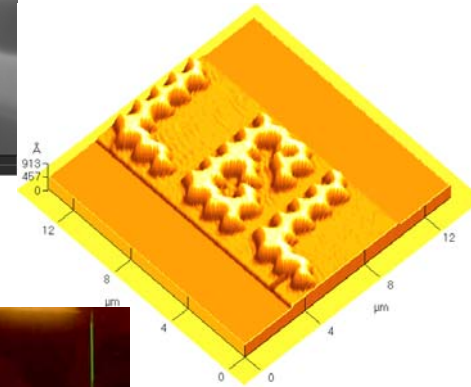
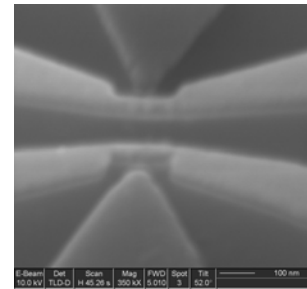
E. O. Lawrence Berkeley National Laboratory

T_Schenkel@LBL.gov

<http://www-ebit.lbl.gov/>

Path to logic demonstrations with donor electron spin qubits in silicon

1. **Develop devices for single spin readout**
 - Spin dependent transport in transistors
2. **Develop a technique for qubit array formation**
 - Single ion implantation with Scanning Probe alignment
3. **Process and materials studies for T_2 optimization**
 - Spin dynamics in pre-device structures
4. **Demonstration of quantum logic**
 - Formulate protocol: requires “only” single spin readout and placement of multiple isotopes into one readout channel

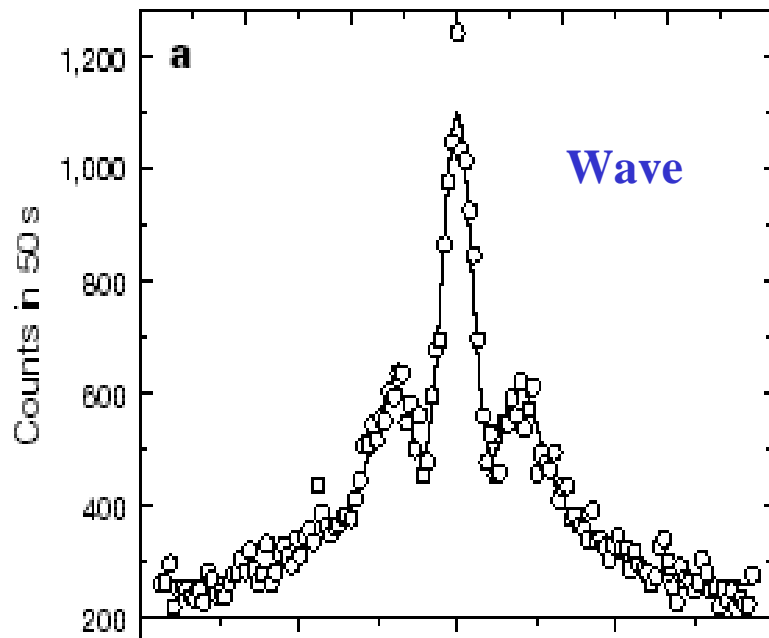


- theory – fabrication – measurement collaboration between LBNL, UC Berkeley (J. Bokor, B. Whaley, R. deSousa), and Princeton University (S. Lyon, A. Tyryshkin)

Wave-particle duality of C_{60} molecules

Wave superposition of states in “double slits” leads to interference
Particle interaction of molecules with environment destroys interference,
 (decoherence, and “classical” behavior)

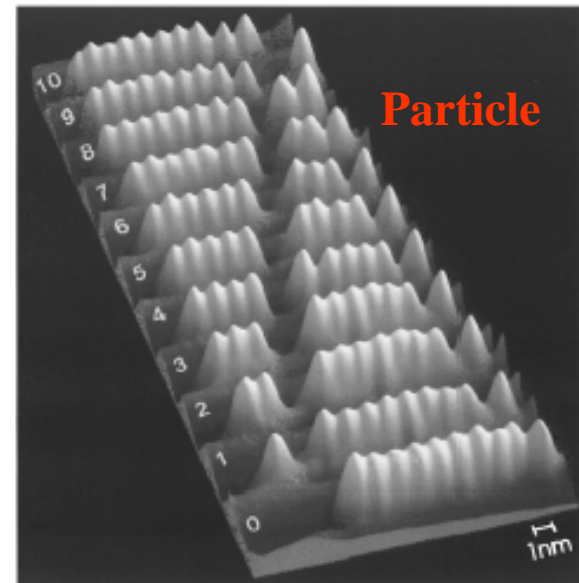
→ Quantum info processing requires the coherent superposition of N qubits!



Markus Arndt, Olaf Nairz, Julian Vos-Andreae, Claudia Keller, Gerbrand van der Zouw & Anton Zeilinger

Institut für Experimentalphysik, Universität Wien, Boltzmanngasse 5, A-1090 Wien, Austria

NATURE | VOL 401 | 14 OCTOBER 1999 |



Room-temperature repositioning of individual C_{60} molecules at Cu steps: Operation of a molecular counting device

M. T. Cuberes,^{a)} R. R. Schlittler, and J. K. Gimzewski
 IBM Research Division, Zurich Research Laboratory, 8803 Rüschlikon, Switzerland

Appl. Phys. Lett. **69** (20), 11 November 1996



Why quantum computation with dopant spins in silicon ?

0. Why Quantum Computation ?

- information storage capacity of N qubits $\sim 2^N$
- quantum algorithms promise speedups
- general paradigm of quantum information theory

1. Why in solids ?

- promise of scalability to large N needed to beat classical computers and including error correction overhead ($N > 10,000$)

2. Why in Silicon ?

- long coherence times for electron and nuclear spins of donor atoms in a silicon matrix
- device requirements converting with trends in classical silicon transistor technology

3. Walk through five DiVincenzo criteria for donor electron spins in Silicon

Why in solids?

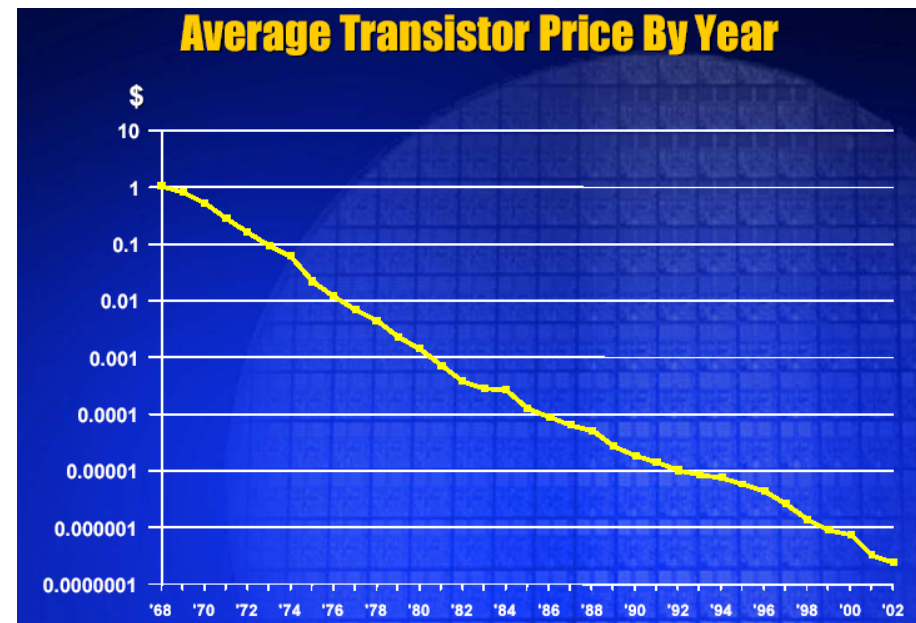
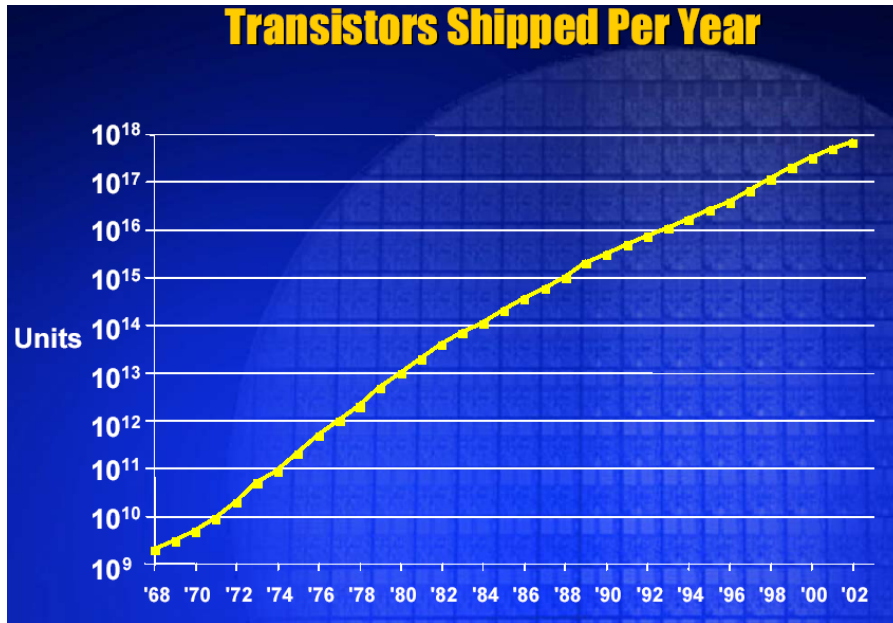
Scalability -

Classical transistor scaling and quantum computer development converge

“Moore’s Law” (Gordon Moore, Intel) exponentially more, cheaper, faster and smaller transistors

more

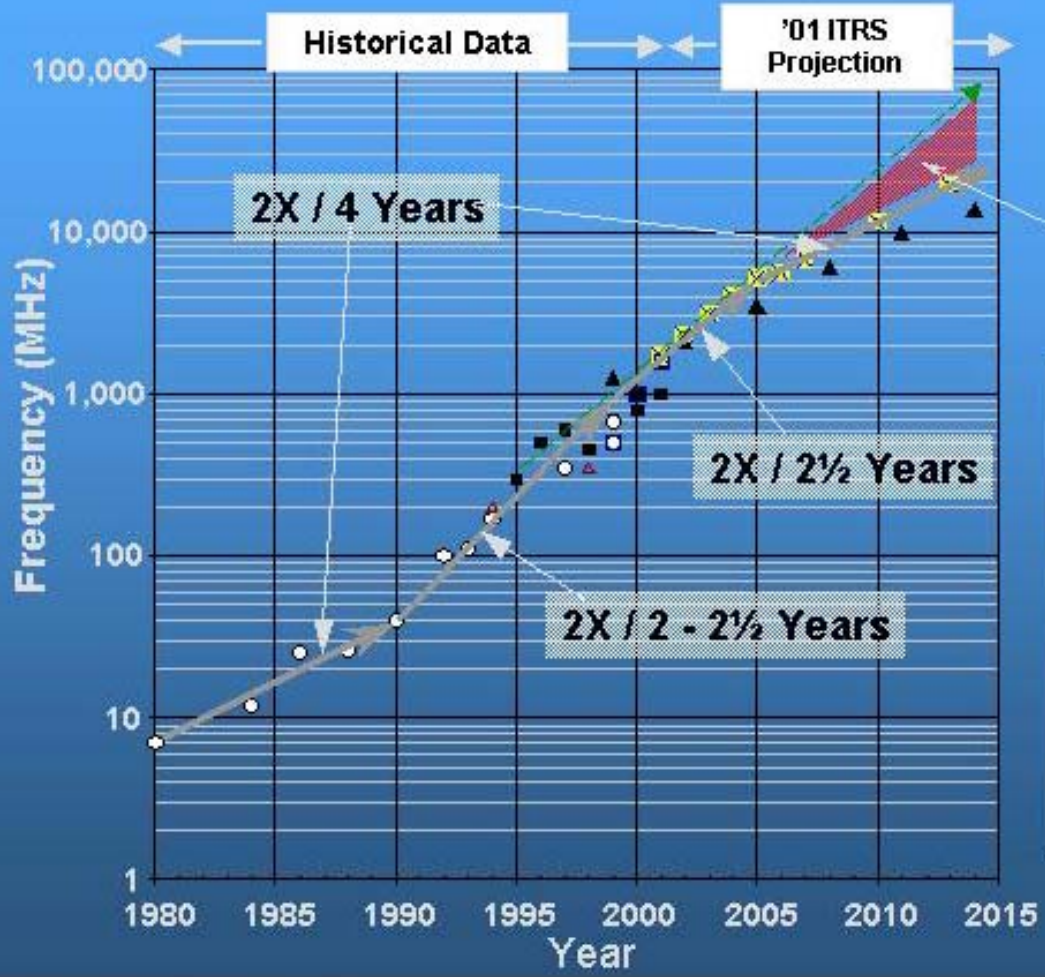
cheaper



As many transistors made each year as raindrops fall on of California
(more then 10 transistors per ant on the planet)

Moore's Law of exponential speedup of silicon transistors: *faster*

Transistor Performance Trend



Innovation needed to maintain historical trend

MPU Clock Frequency Historical Trend:

Transistor scaling has contributed ~ 17-19% / year

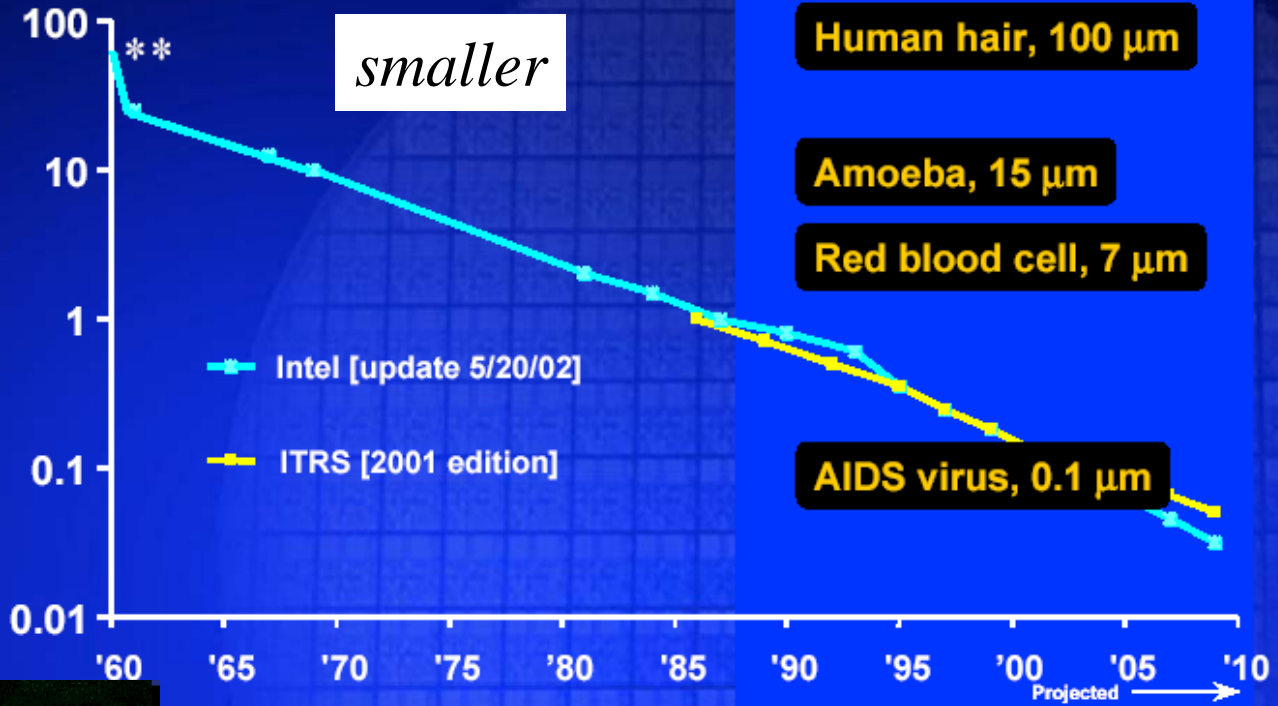
Architectural Design innovation contributed additional ~ 13-21% / year

Sources: SEMATECH, 2001 ITRS ORTC

$f = 1/\tau = I/CV$; τ = delay; one transistor's gate load capacitance

Minimum Feature Size

Feature Size (microns)



Examples

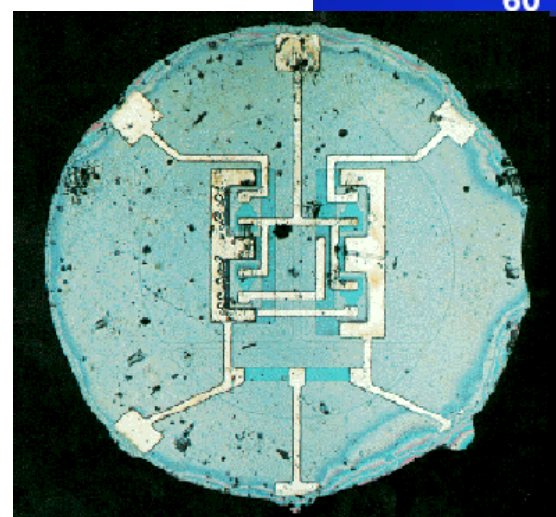
Human hair, 100 μm

Amoeba, 15 μm

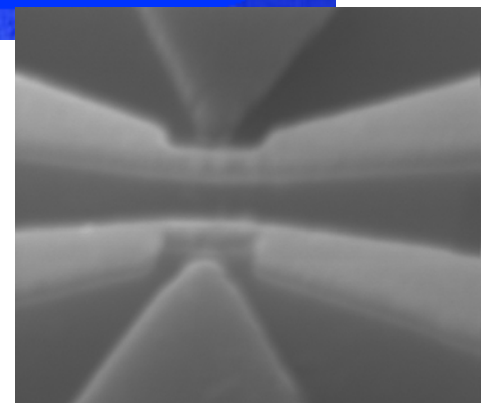
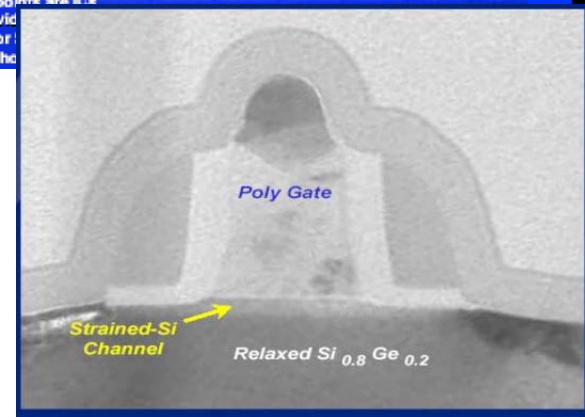
Red blood cell, 7 μm

AIDS virus, 0.1 μm

Buckyball, 0.001 μm



...g data points are ICs
...data provid
...admap for:
...Intel "Litho



E-Beam	Det	Scan	Mag	FWD	Spot	Tilt	100 nm
10.0 kV	TLD-D	H 45.26 s	350 kX	5.010	3	52.0°	



Why silicon ?

- **vastly abundant semiconductor that is “easy” to work with**
 - SiO₂ / Si interface has quite low defect density
 - ($\leq 10^{10}$ cm⁻²eV⁻¹, that’s still ~ 1 per 100 nm scale device)
 - very high degree of control over electrical properties
 - allows large scale integration
 - most importantly: **very long coherence times** (> 1 ms)
 - because it can be prepared as a nuclear spin free environment (pure ²⁸Si)
- compared to other materials with specific advantages:
 - **III-V’s, e. g., quantum dots in GaAs**
 - direct band gap for opto-electronic integration
 - very high quality 2DEGs
 - but: short coherence times, ~ 1 μ s, due to nuclear spin flips
 - **diamond** (e. g., NV defects):
 - larger band gap for high temperature operation
 - low spin orbit coupling
 - but difficult to make larger wafers, hard to dope, ...
 - **electrons on liquid helium, endohedral C60, ...**

Donor electron spin qubits in silicon

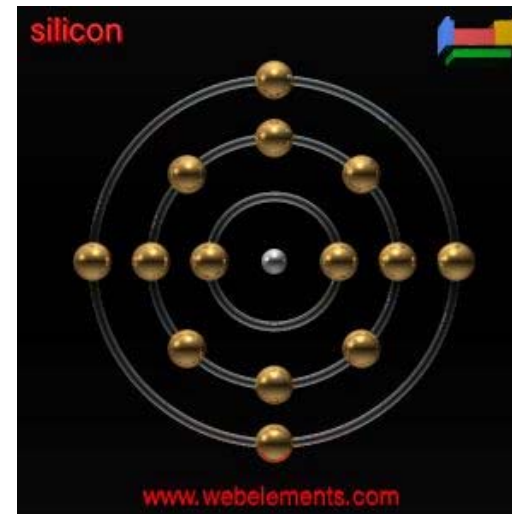
5 B BORON 11	6 C CARBON 12	7 N NITROGEN 14
13 Al ALUMINUM 27	14 Si SILICON 28	15 P PHOSPHORUS 31
31 Ga GALLIUM 70	32 Ge GERMANIUM 73	33 As ARSENIC 75
49 In INDIUM 115	50 Sn TIN 119	51 Sb ANTIMONY 122
81 Tl THALLIUM 204	82 Pb LEAD 207	83 Bi BISMUTH 209

^{31}P (natural quantum dot)

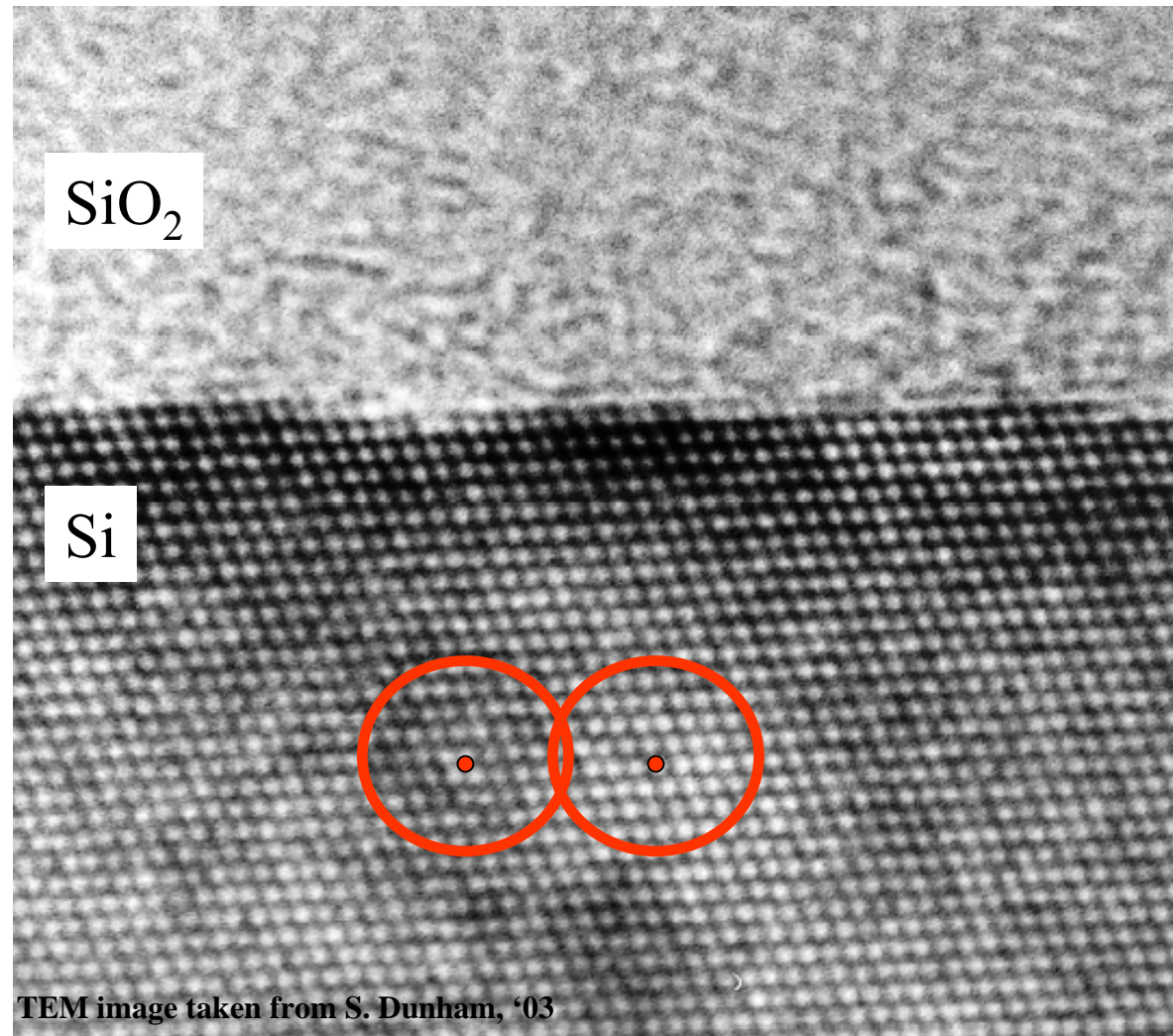
Si: $[\text{Ne}].3s^2.3p^2$

P: $[\text{Ne}].3s^2.3p^3$

- $3p^3$ binding energy: 45 meV
- 100% abundant isotope with $I=1/2$
- ^{28}Si matrix can be prepared with $I=0$



Qubit: spins of ^{31}P atoms in silicon



- Long decoherence times
 - nuclear spin: ~ 1000 s
 - electron spin: tens of ms

- Bohr radius of bound, 3p electron of ^{31}P in Si: ~ 2 nm

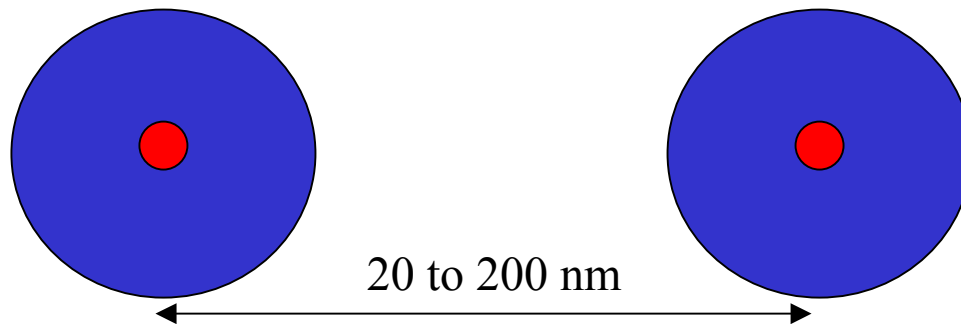
$$a_0 = \epsilon_{Si} \frac{m_0}{m_{eff}} \epsilon_0 \frac{h^2}{\pi m_0 q^2} =$$

$$= \epsilon_{Si} \frac{m_0}{m_{eff}} 0.53 \text{ \AA}$$

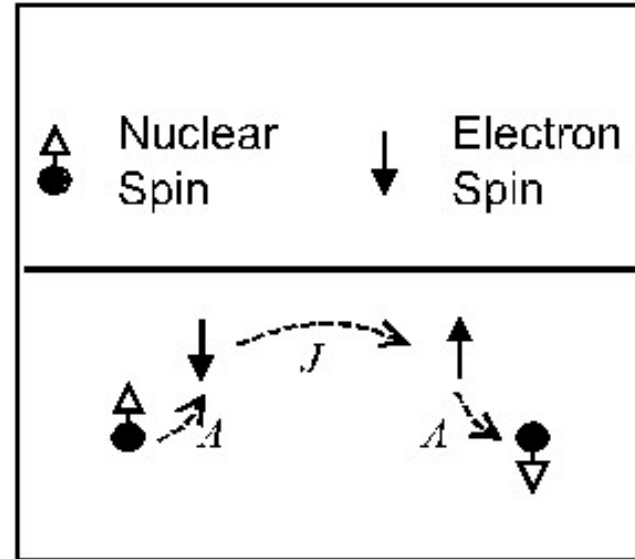
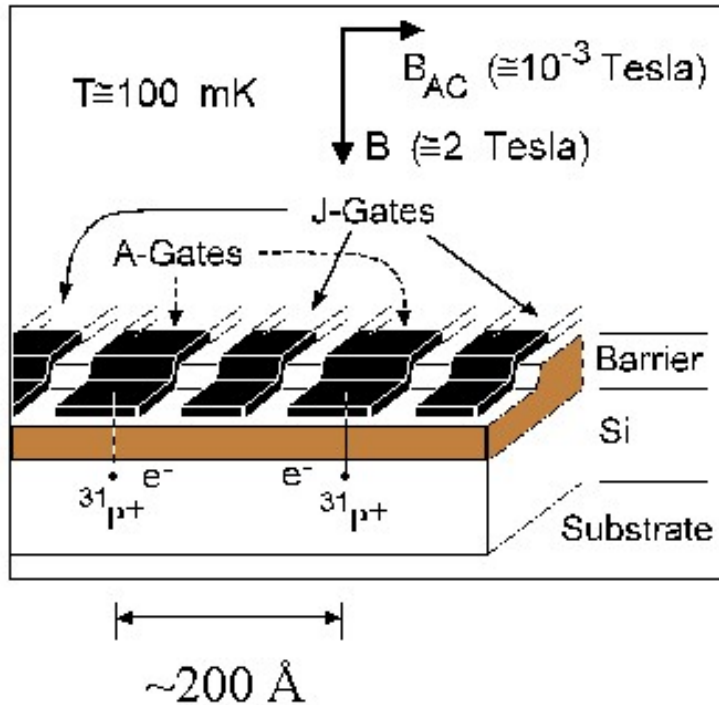
$$(\epsilon_{Si} = 12)$$

1. Well defined extendible qubit array – stable memory
2. Initialization in the “000...” state
3. Long decoherence time ($>10^4$ operation time, to allow for error correction)
4. Universal set of gate operations (not, cnot)
5. Read-out: Single-quantum measurements (projective measurement)
6. Efficient quantum communication (form, transmit and convert “flying qubits”)

^{31}P donor spins in silicon: “natural quantum dots”



Solid state quantum computer scheme with ^{31}P in ^{28}Si (B. E. Kane, Nature 1998)



- ^{31}P -qubit: gate controlled manipulation of single spins; nuclear spins store information, electron spins transfer information between neighboring qubits (J , exchange) and to nuclear spins ($A=121.5 \text{ neV}$, hyperfine interaction) (<http://www.lps.umd.edu/>)

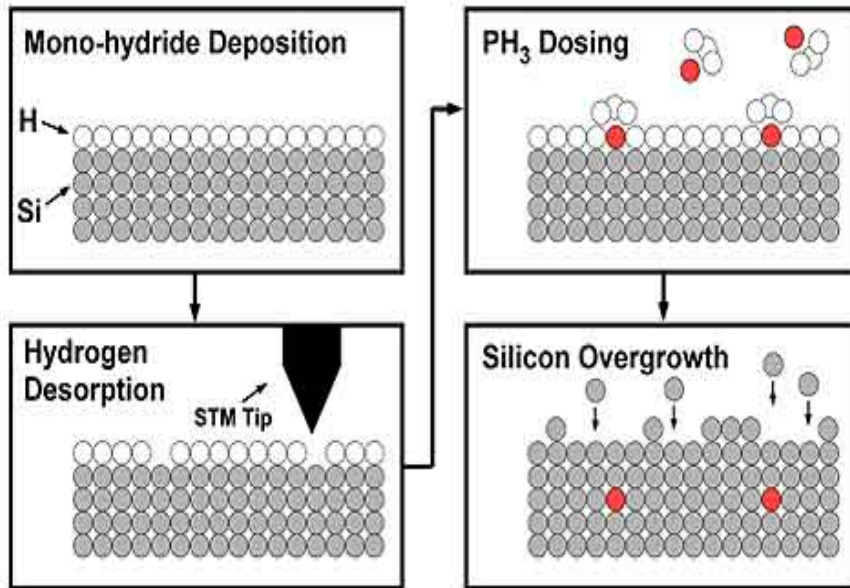


Criteria for physical implementation of a quantum computer

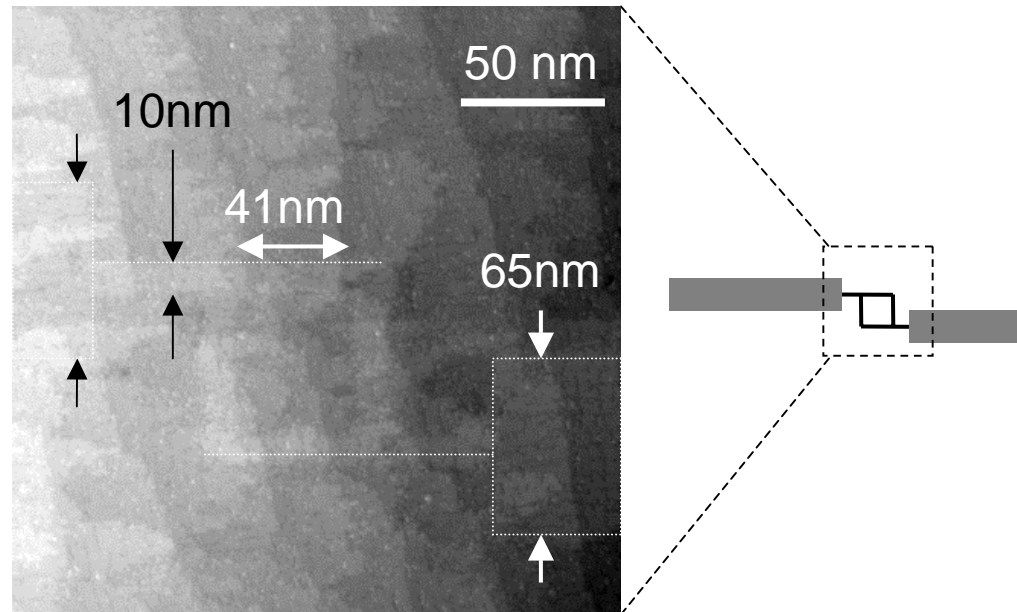
(DiVincenzo)

1. **Well defined extendible qubit array – stable memory**
 - **Array of single donor atoms (P, As, Sb, Bi) in a silicon crystal matrix formed by single ion implantation (or STM-H lithography)**
2. Initialization in the “000...” state
 - polarization at low temperature (0.3 K), in strong magnet field (5 T), $kT \ll g\mu_B B$
3. Long decoherence time ($>10^4$ operation time, to allow for error correction)
 - $T_2 = T_1$ in pure ^{28}Si >10 s, limited by residual ^{29}Si , and by gate, and interface effects
4. Universal set of gate operations
 - Not: ESR rotations, need local B or g control
 - CNOT: two qubit interaction via J, or dipolar coupling, or RKKY, or e^- shuttling
5. Read-out (projective measurement)
 - Single shot, single spin readout, much faster than decoherence time
 - spin-to-charge conversion, spin dependent transport

Qubit arrays bottom up: STM hydrogen lithography



J. O'Brien, et al.,
Univ. New South Wales, Sydney



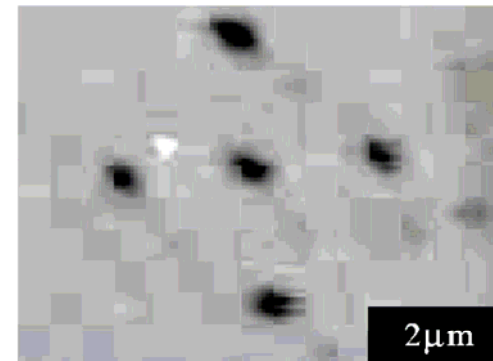
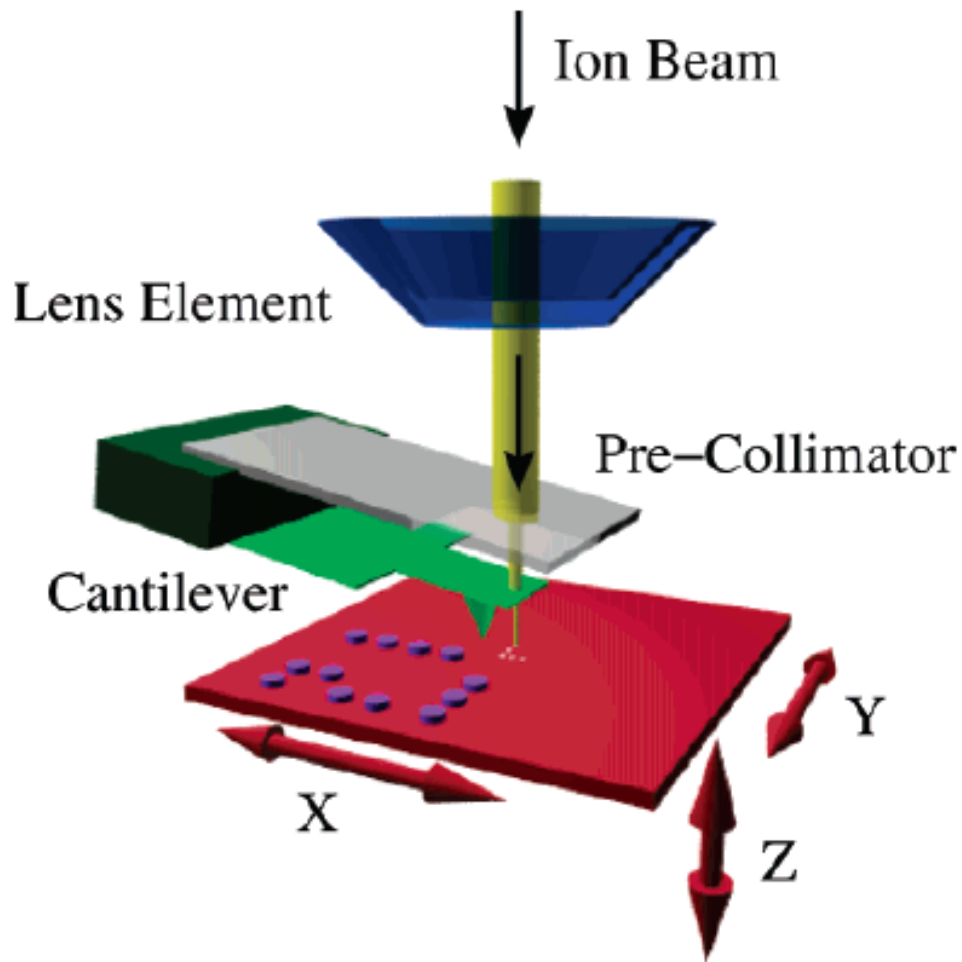
Aharonov-Bohm ring of P atoms connected to pre-implanted contacts, and overgrown with Si on Si (100); TC. Shen, J. Tucker, et al., 2003

- Desorption of H with low energy electrons (~ 10 eV) from the STM tip
- Advantage: atomic resolution
- Problems: encapsulation, dopant activation, device integration, surface chemistry sensitivity

Single Ion Implantation

1) Ion Placement

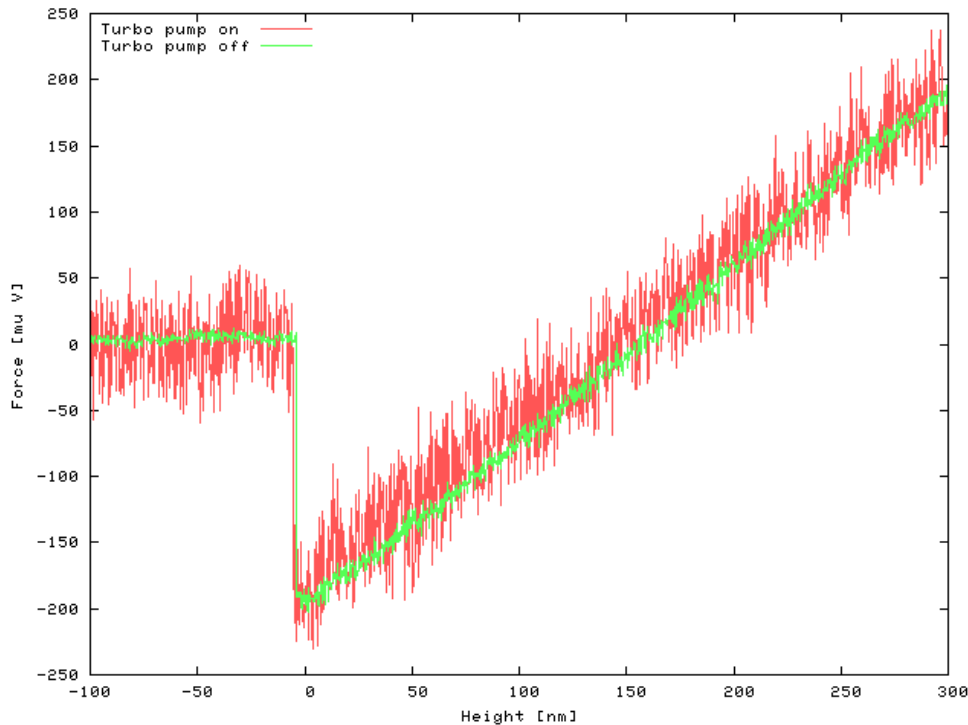
Goal: place single ions with nm resolution



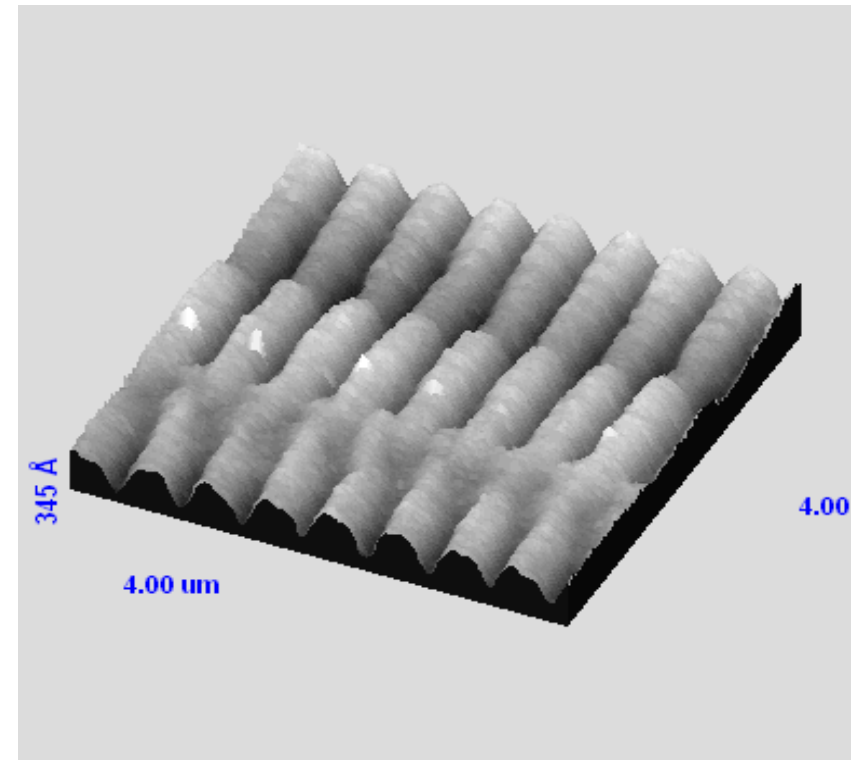
**A. Persaud, et al.,
Nano Letters 5, 1087 (2005)**

Scanning Probe connected to ion beam line allows imaging and alignment with nanometer resolution

(~5 nm with turbos on, ~0.5 nm RMS with turbos off)

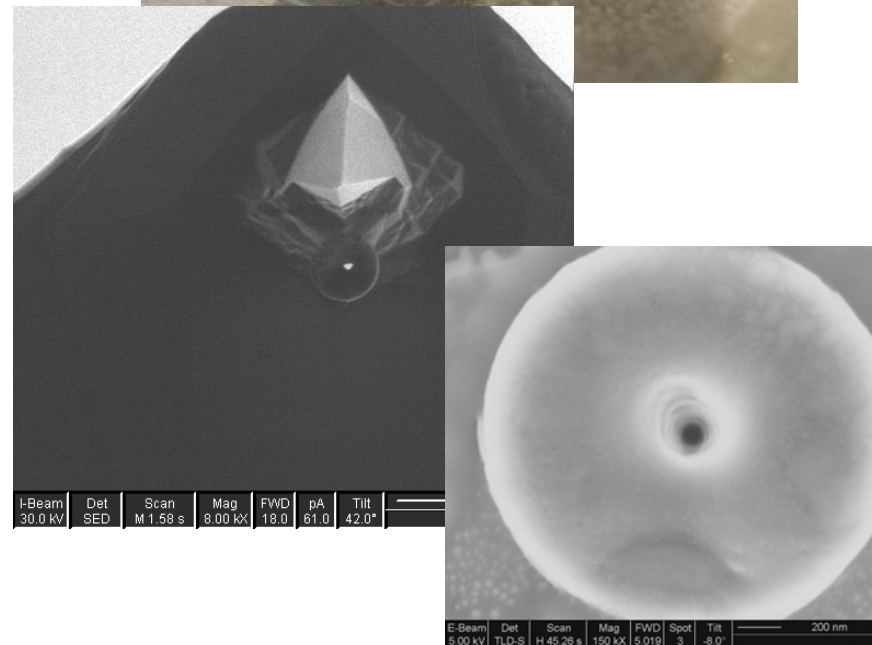
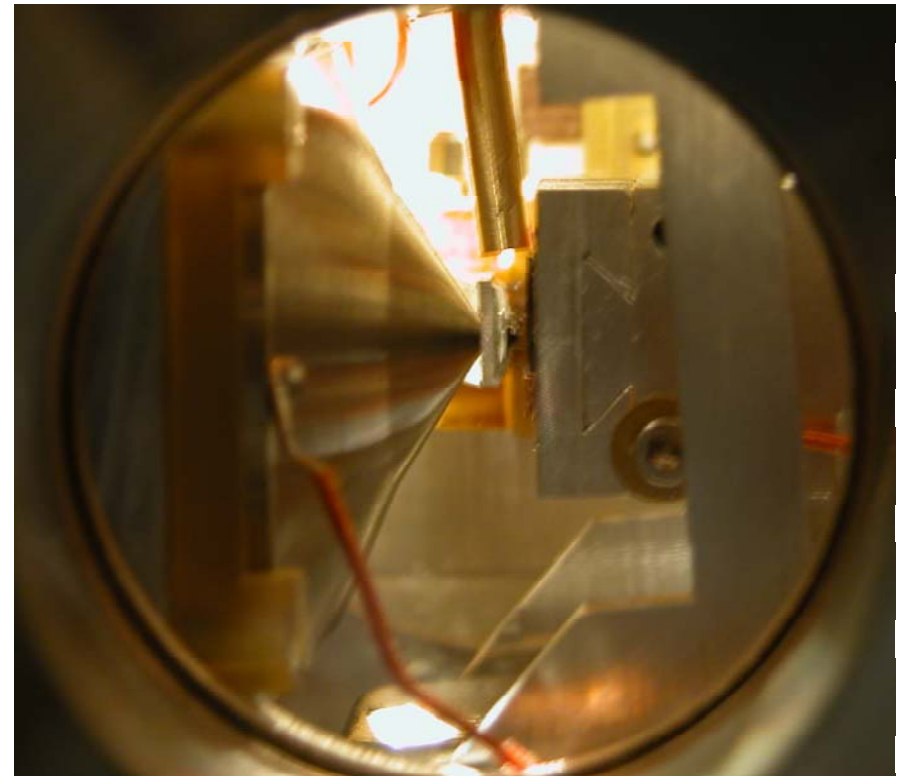
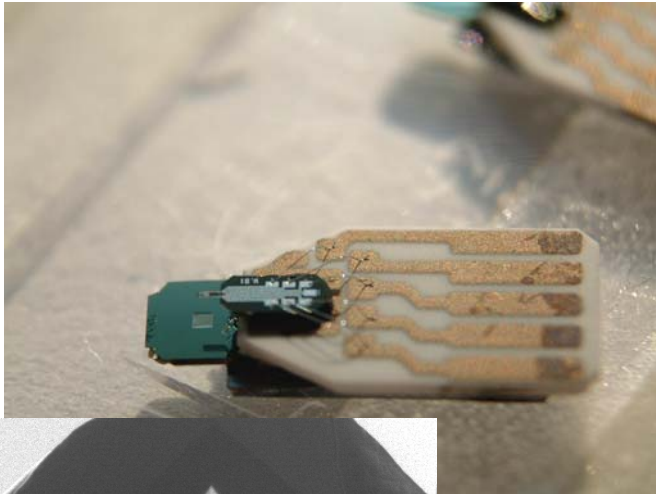


- force (μV) vs. distance (nm) curves from piezo AFM in situ with turbos on and off



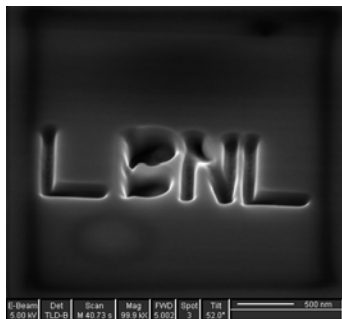
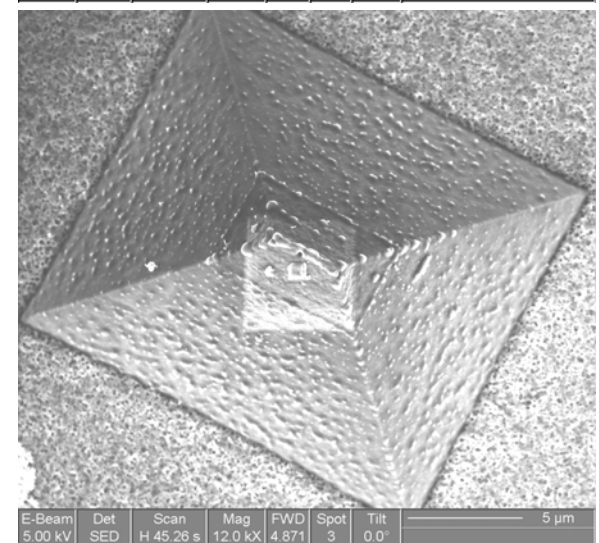
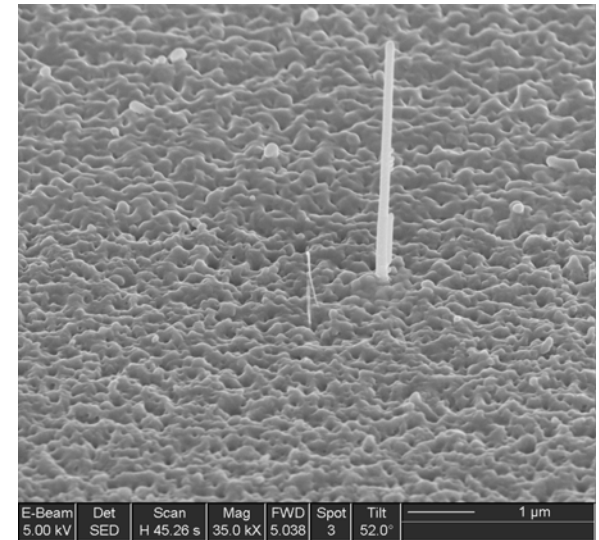
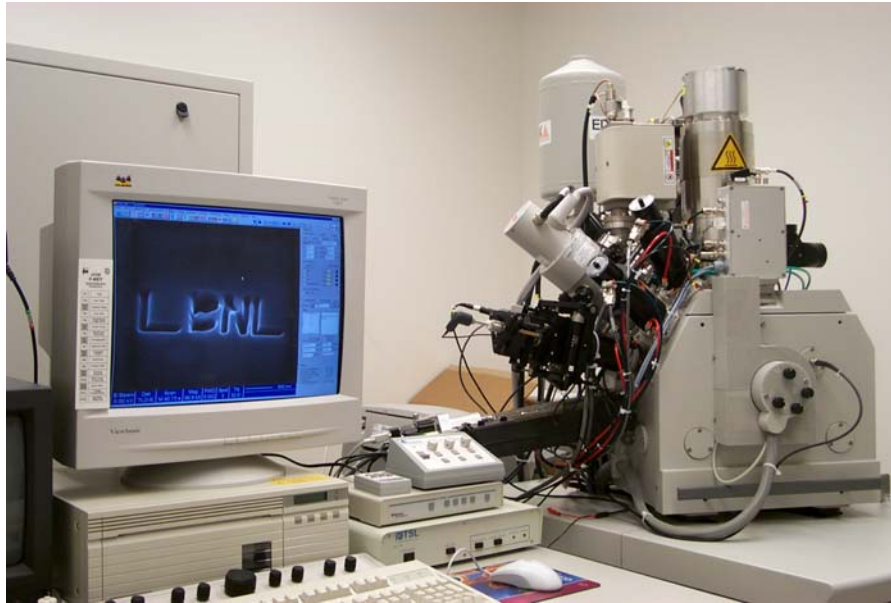
- *in situ* Scanning Probe images of imprint stripes (50 nm trenches, right)
- stripes by S. Kwon, Molecular Foundry, LBNL

Single Ion Implantation with Scanning Probe alignment

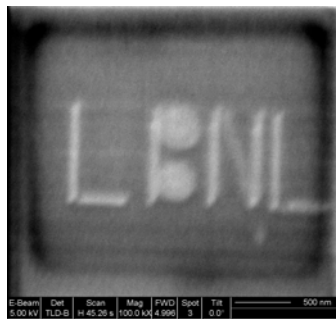


- SII-SPM setup connected to high vacuum beam line
- scan range of target stage is $0.1 \times 0.1 \text{ mm}^2$
- probe tip can be moved across 1 mm field
- piezo-cantilevers co. I. Rangelow, Kassel University

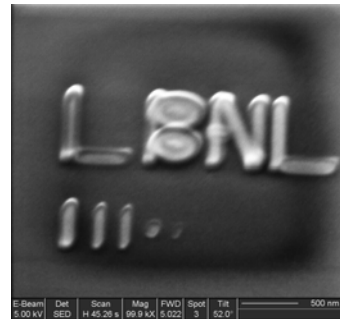
FEI Strata 235 dual beam FIB at LBNL



etching

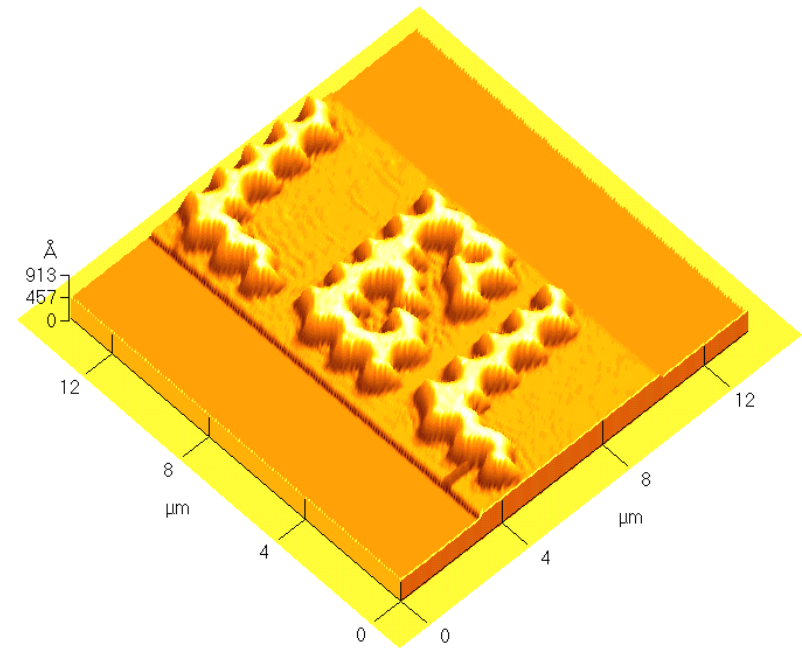
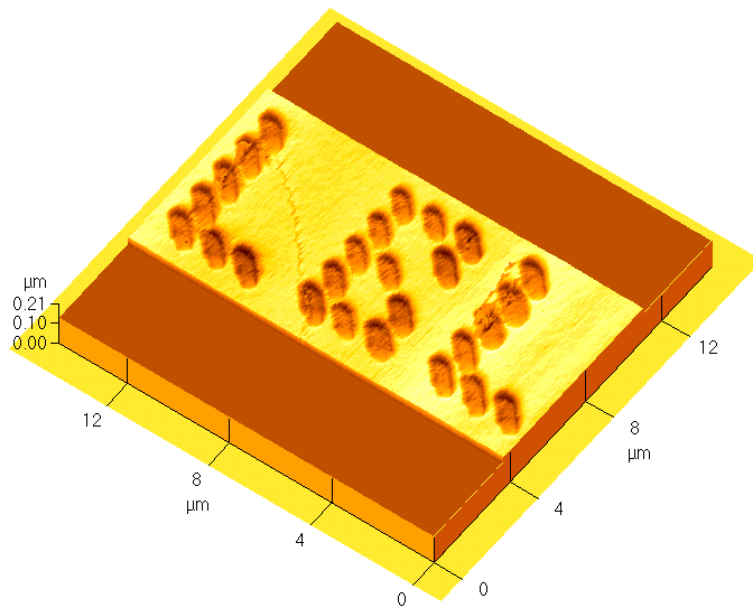


oxide deposition



Pt deposition

Integration of Ion Beam and Scanning Probe - Patterning by transport of ions through holes in a scanning probe tip

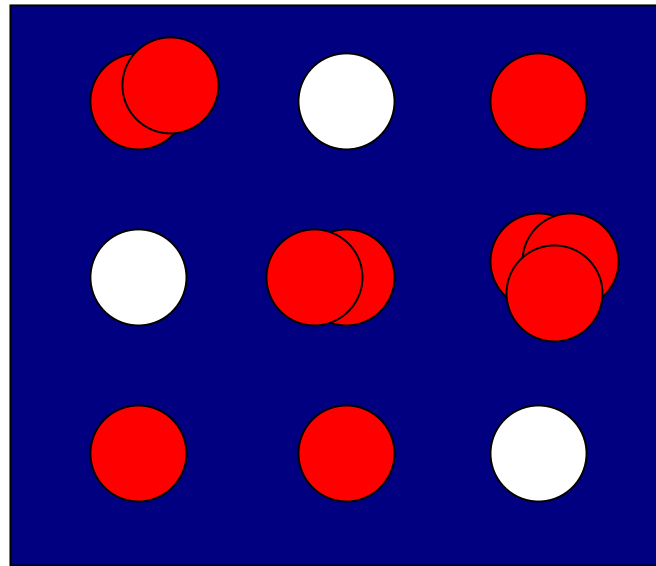


- dot array formed by Ar^{2+} (7 keV) in PMMA (poly-methyl-methacrylate, positive resist)

- dot array formed by Ar^{2+} in HSQ (hydrogen silsesquioxane, negative resist)

- ion placement resolution is limited by hole size, work with <80 nm holes is in progress

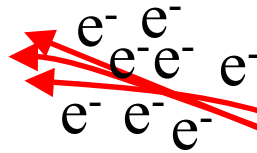
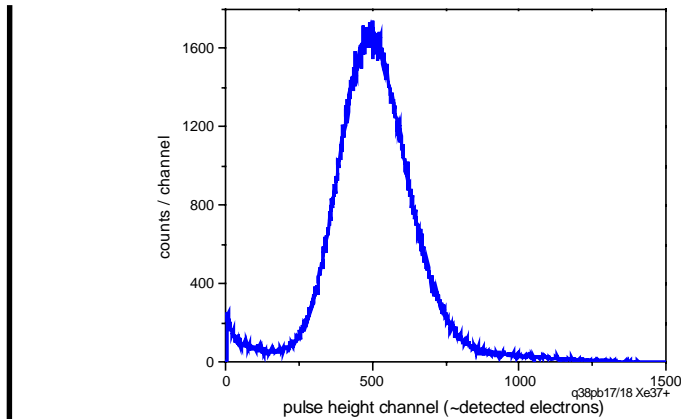
Poissonian distribution of implanted ions



- Distribution of probabilities for implantation of ions where the implantation probability is small ($\ll 1$) for each incident ion and the number of ion impacts is large ($\gg 1$)
- At average, one ion is implanted. The probability for two adjacent ion hits is 13%

Qubit arrays top down: Single Ion Implantation with Scanning Probe Alignment

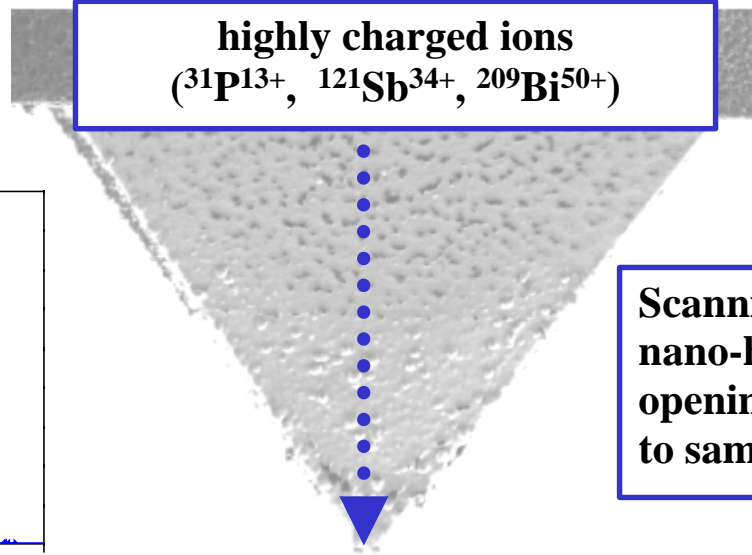
beam is blocked following one event and sample is moved to next qubit site



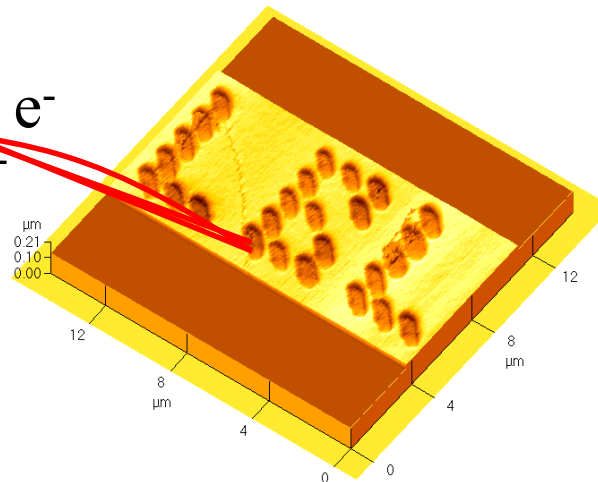
detection of multiple secondary electrons from single ion hits registers single ion impacts

(components not to scale)

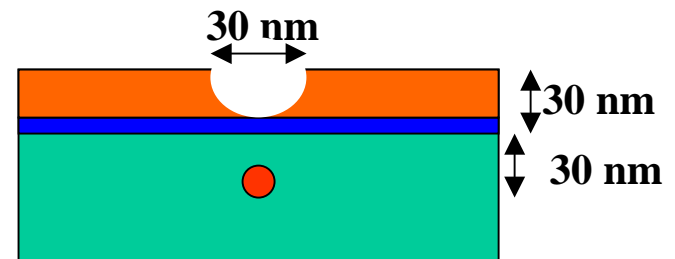
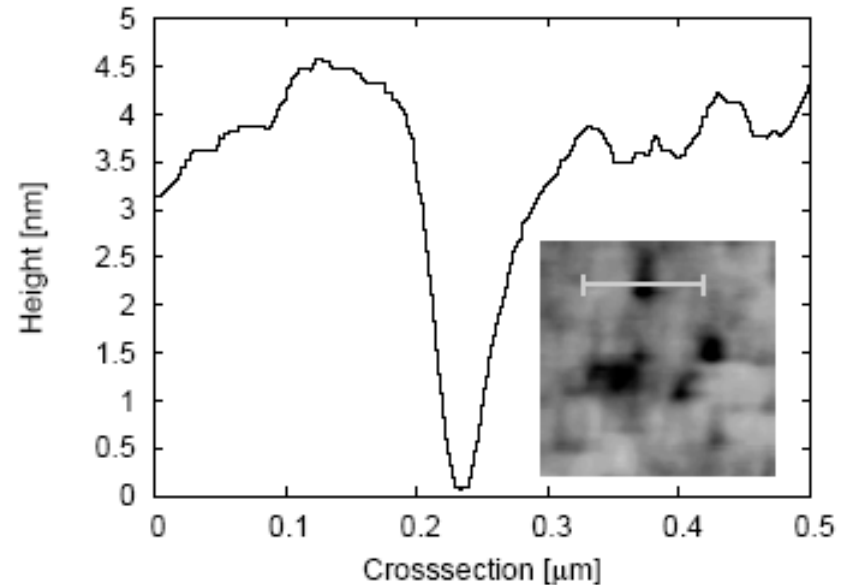
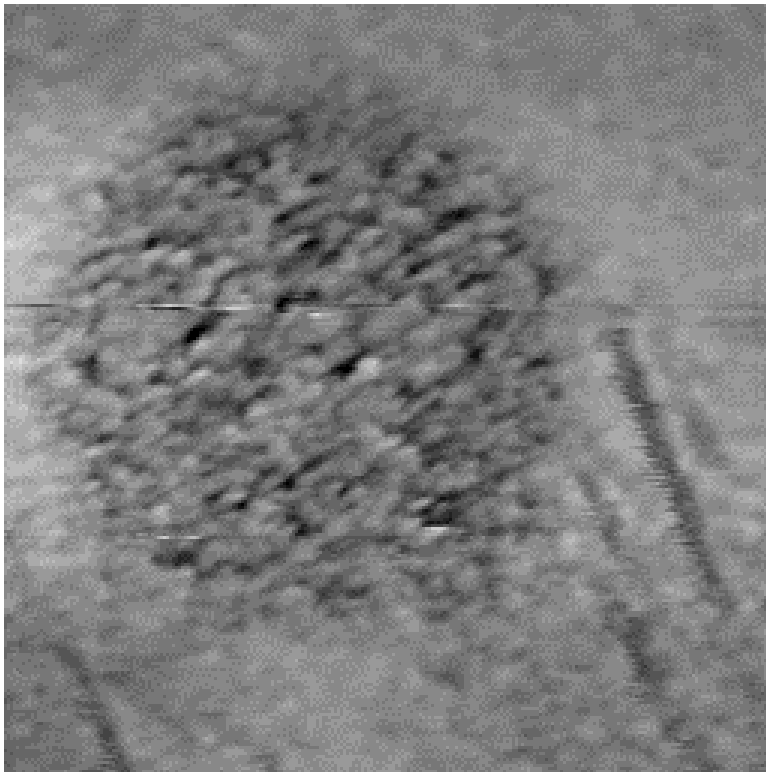
highly charged ions
($^{31}\text{P}^{13+}$, $^{121}\text{Sb}^{34+}$, $^{209}\text{Bi}^{50+}$)



Scanning Probe with nano-hole (down to 5 nm opening) aligns ion beam to sample features

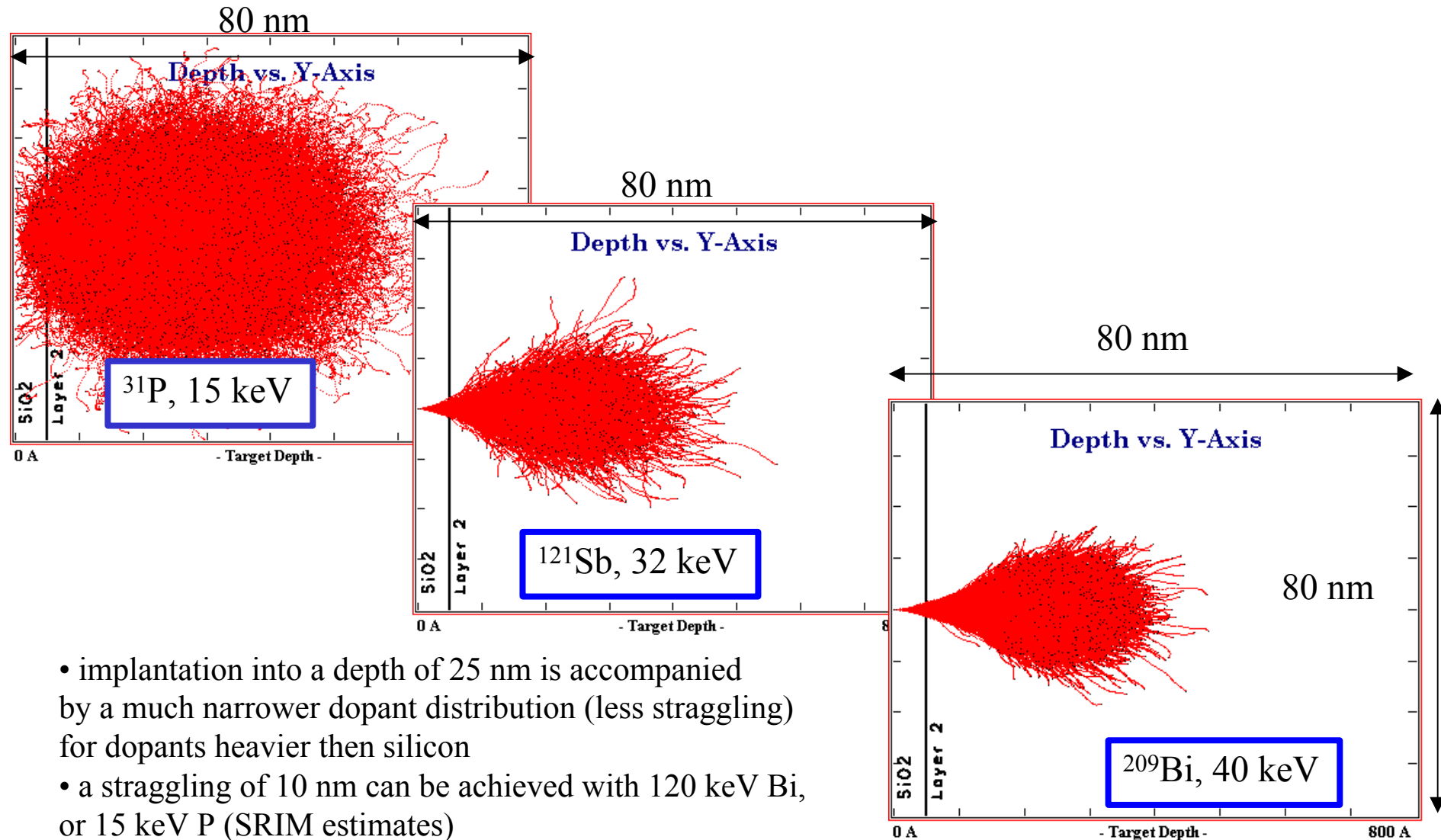


Single ion impact sites in resist layers



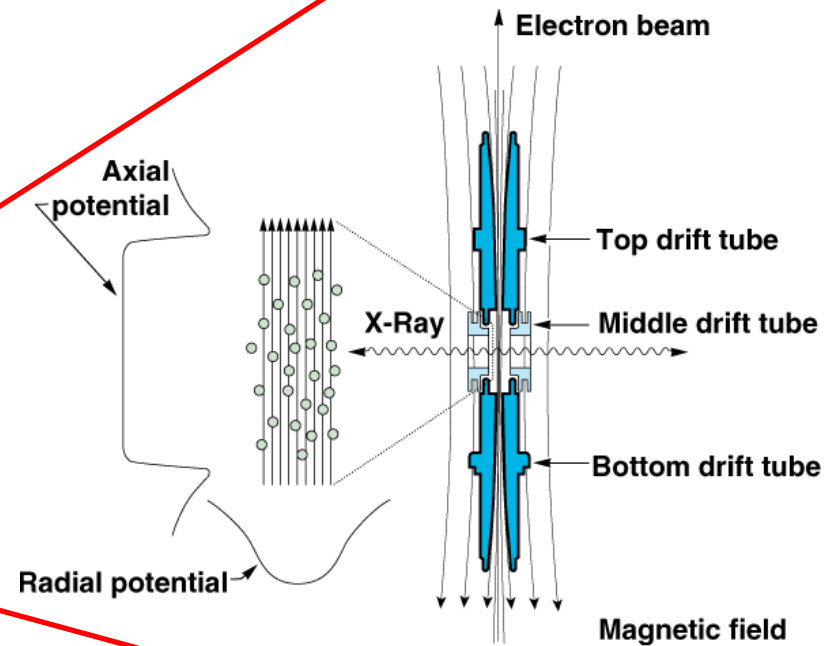
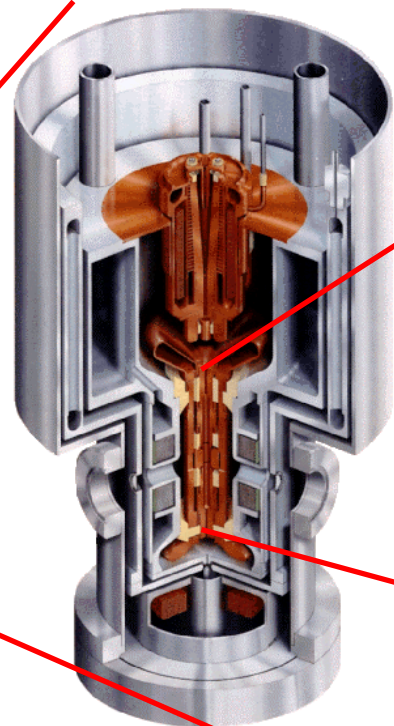
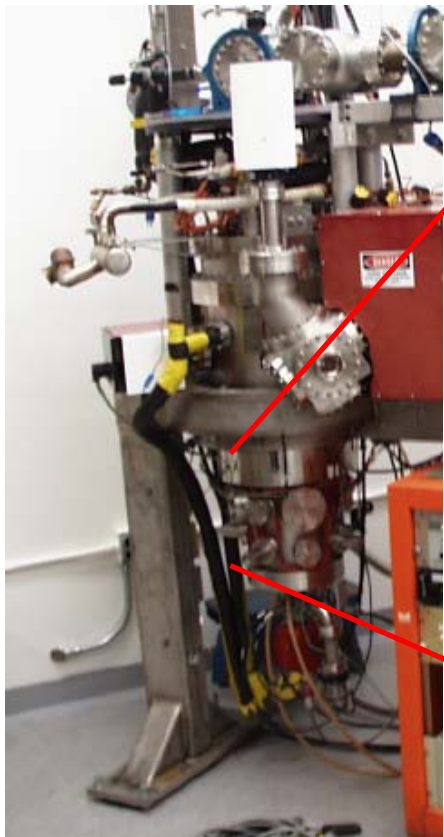
- Left: *Ex situ* scanning probe image of a 2 μm wide spot where PMMA was exposed to Xe³⁰⁺ ions (180 keV).
- Right: image and line out of a Bi⁴⁵⁺ single ion impact site after resist development.

Scattering kinematics favours implantation of heavy donors into Si



- implantation into a depth of 25 nm is accompanied by a much narrower dopant distribution (less straggling) for dopants heavier than silicon
- a straggling of 10 nm can be achieved with 120 keV Bi, or 15 keV P (SRIM estimates)

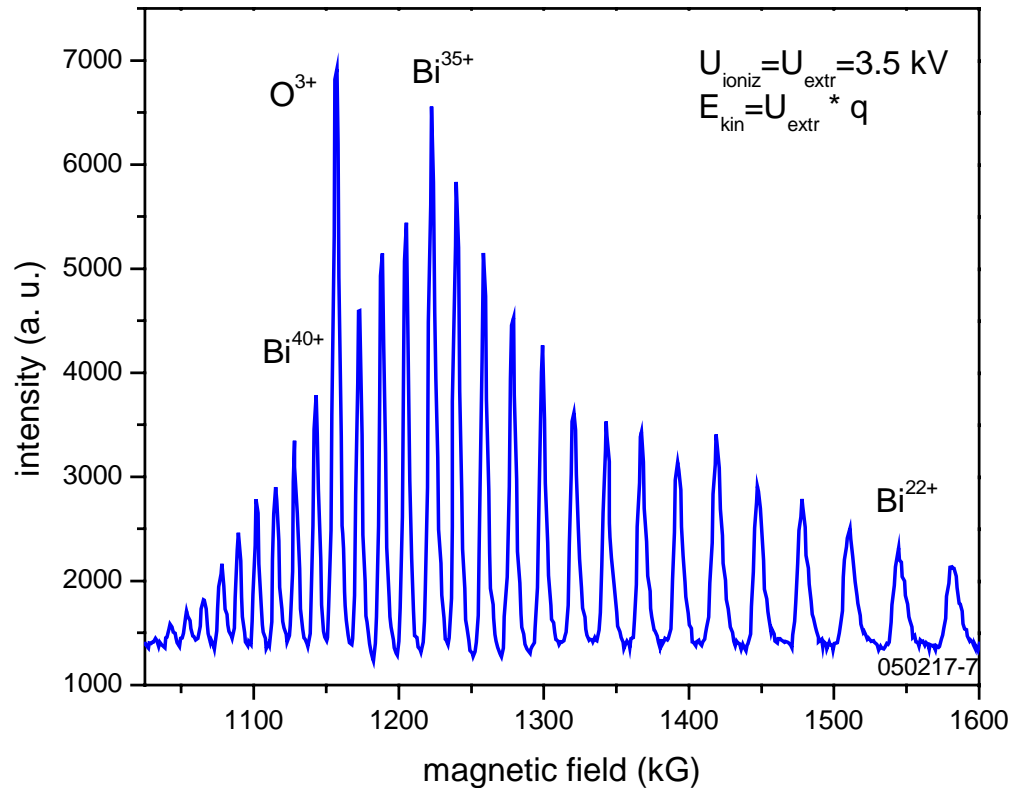
The Electron Beam Ion Trap - a source for slow ($v < v_0$), highly charged ions



- beams of highly charged ions like P^{15+} , Ni^{26+} , As^{31+} , Sb^{41+} and Bi^{60+} and kinetic energies from as low as 100 eV (with deceleration) up to 1 MeV

Single Ion Implantation - Ion Detection

High charge states make low energy ions “visible”



- which donor species is best ?
- ^{31}P is a common impurity, and we can avoid ambiguities by using other donors
- scattering kinematics favors heavy projectiles for minimal straggling

- **High charge states enhance signal for single ion detection**

1. Secondary electron emission

- Phys. Rev. Lett. 68, 2297 (1992)
- Most universal, requires pyramid tip

2. Electron-hole pairs in solids

- Phys. Rev. Lett. 83, 4273 (1999)
- Requires transistor, ideal if you have one

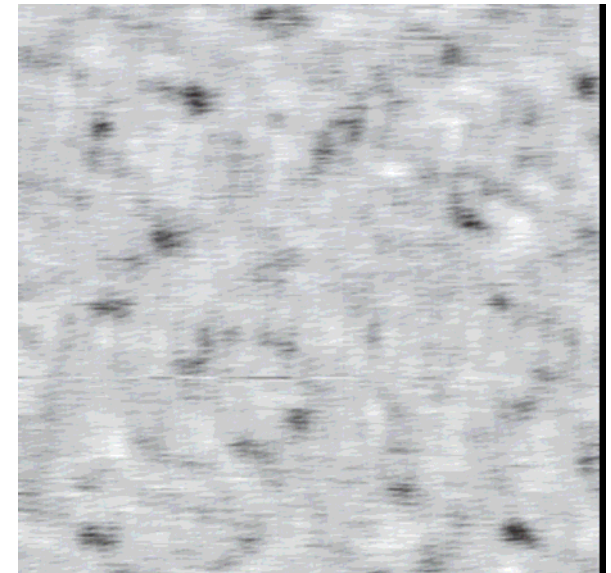
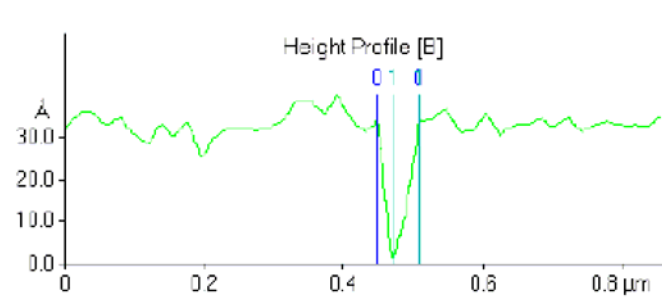
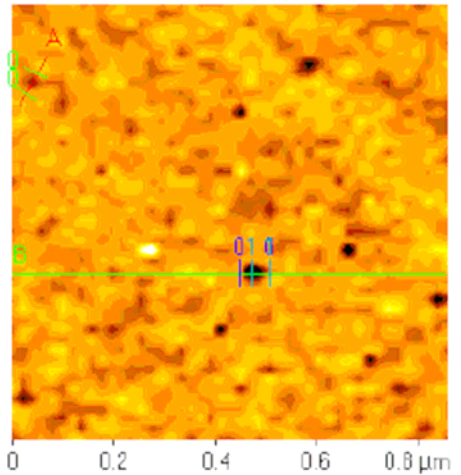
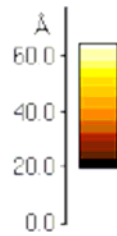
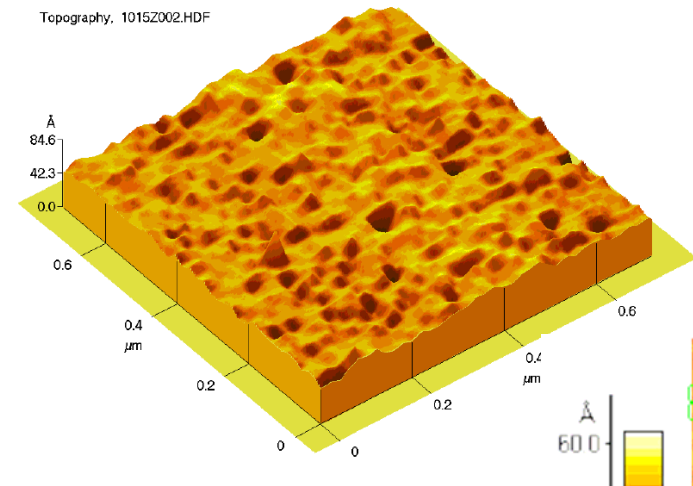
3. Topography modifications

- J. Vac. Sci. Technol. B 16, 3298 (1998)
- Requires insulating surface and high resolution *in situ* imaging

Single ion impact detection via topography modifications

-works well for flat surfaces on insulators, and high resolution *in situ* imaging

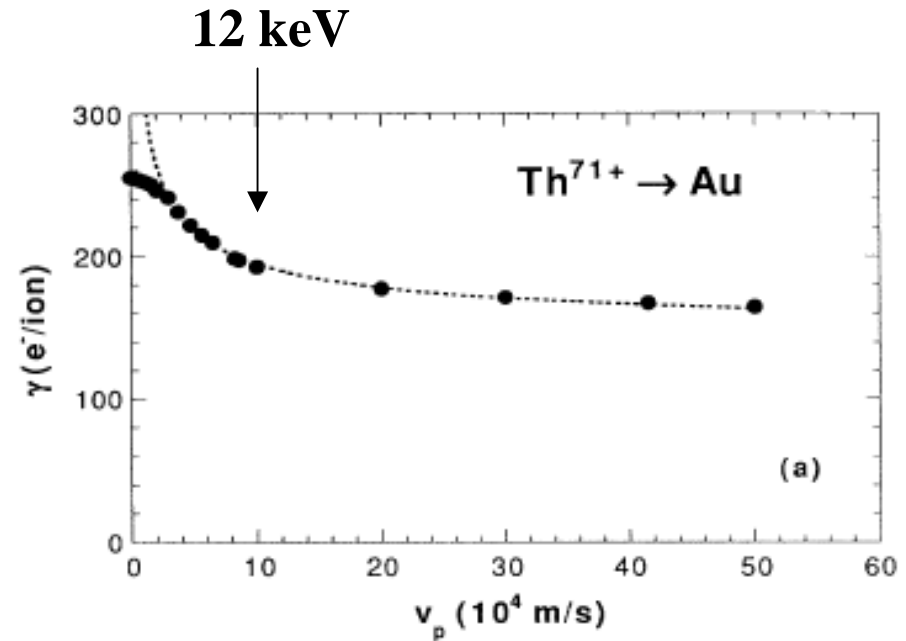
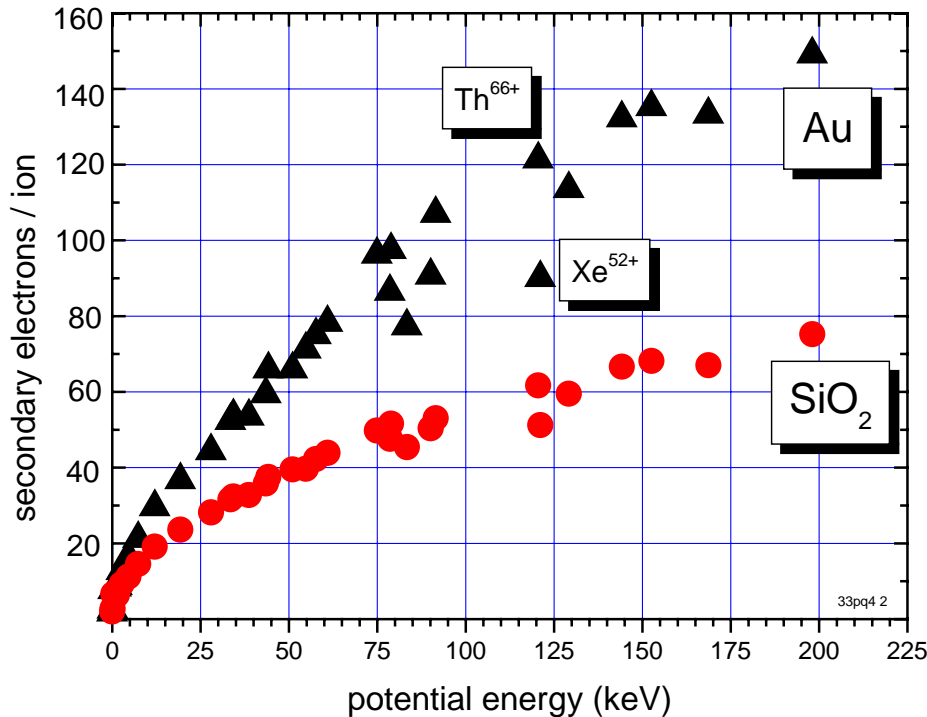
Topography, 1015Z002.HDF



- ~15 nm wide crater in float zone silicon (*ex situ*), from single Xe⁴⁴⁺ impacts, Appl. Phys. A 76, 313–317 (2003)

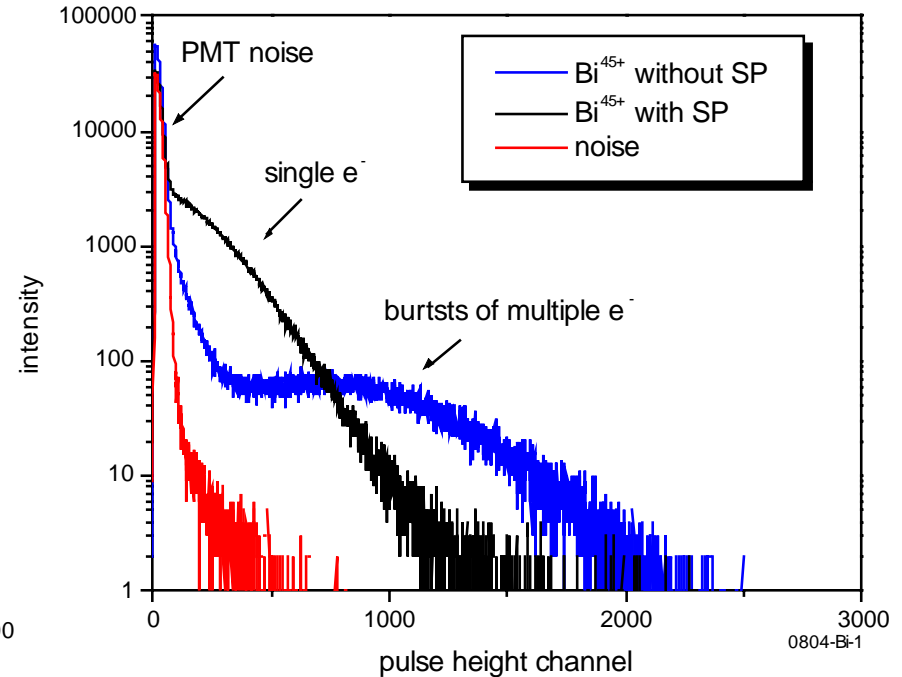
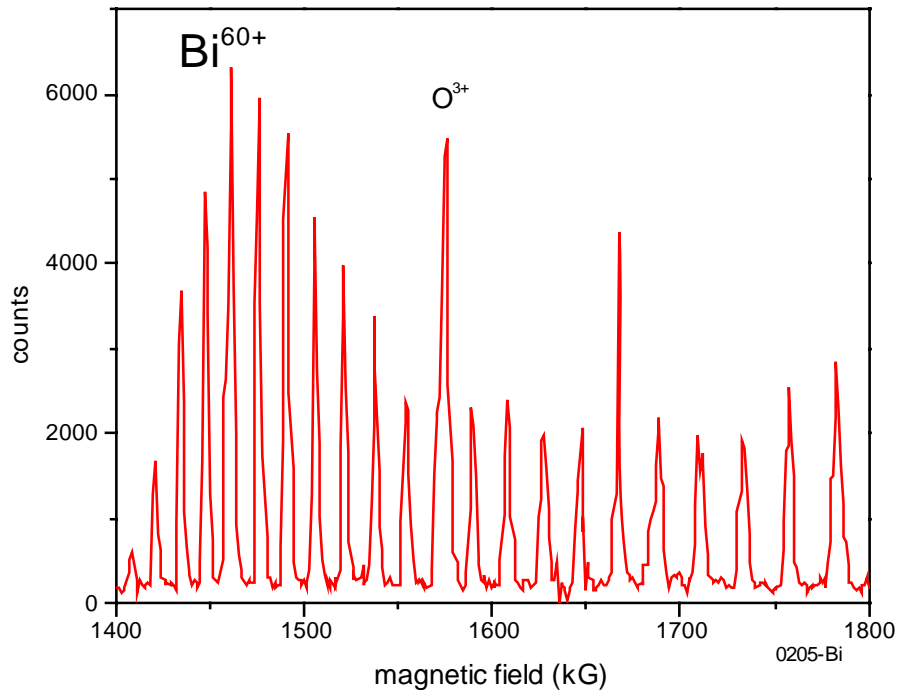
- Xe⁴⁰⁺ induced defects, ~50 nm wide, in diamond (nicely polished, ~ 1 nm RMS), (*ex situ*, image from E. Haddad)

Emission of secondary electrons by low energy (<3 keV/u) highly charged ions



- Left: Secondary electron yields from gold and SiO₂ (150 nm on Si) vs. E_{pot} of highly charged ions (Xe, Au and Th) with kinetic energies of $9 \text{ kV} \times q$ (Schenkel et al., NIM B 125, 153 (1997)). Yield from SiO₂ is lower due to local charging in single impact events.
- Right: Secondary electron yields vs. impact velocity for Th⁷¹⁺ on Au (Aumayr et al. PRL 71, 1943 (1993))

Detection of $^{209}\text{Bi}^{45+}$ ions with Scanning Probe in place



- ^{209}Bi implantation:
- less straggling for placement into given depth (factor two compared to P),
- smaller diffusion coefficient (factor 10)
- compatible with SiO_2 (due to vacancy mediated diffusion)
- but more damage (anneals well, aiding activation)

- electron collection in presence of Scanning probe tip has to be further optimised
- the experiment was sub-optimal, since both the scintillator and the PMT used for electron detection had deteriorated accidentally
- with new scintillator and PMT, we can separate single electron noise (hits on apertures) from ion hits on the sample

Single ion detection by tracing of potential energy from high charge states inside a transistor

VOLUME 83, NUMBER 21

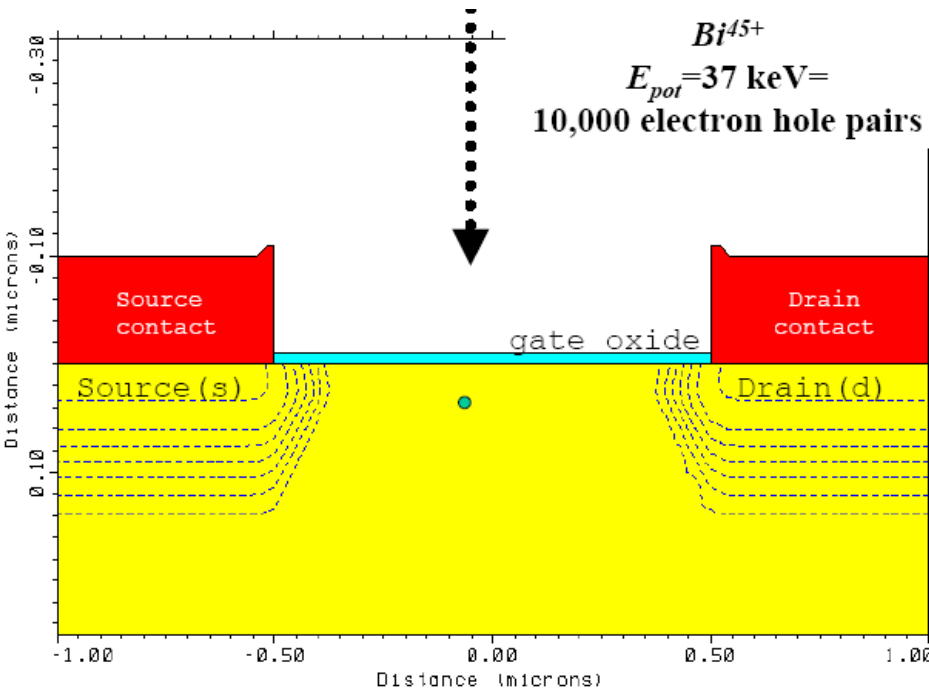
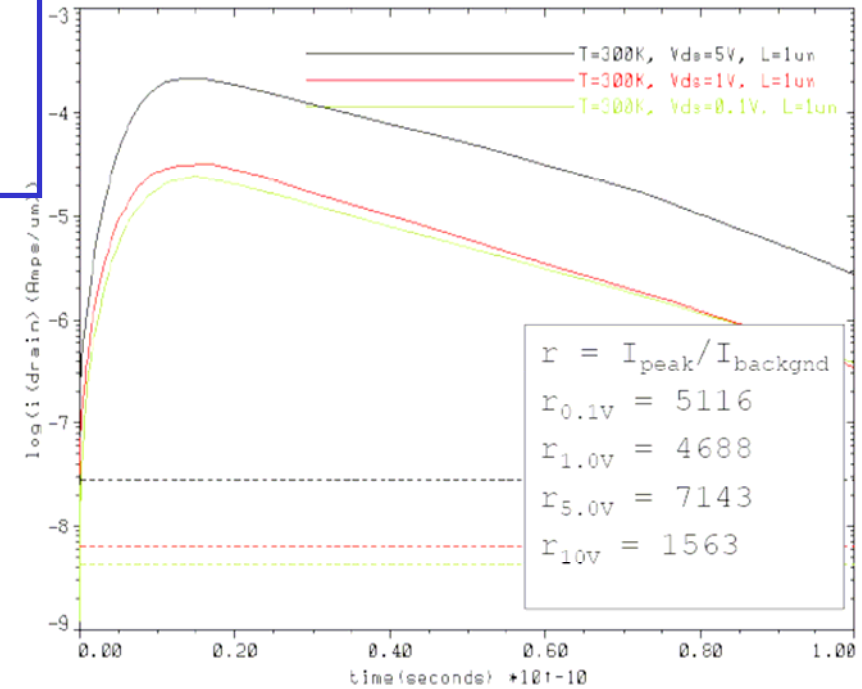
PHYSICAL REVIEW LETTERS

22 NOVEMBER 1999

Deposition of Potential Energy in Solids by Slow, Highly Charged Ions

T. Schenkel,* A. V. Barnes, T. R. Niedermayr, M. Hattass, M. W. Newman,
G. A. Machicoane, J. W. McDonald, A. V. Hamza, and D. H. Schneider

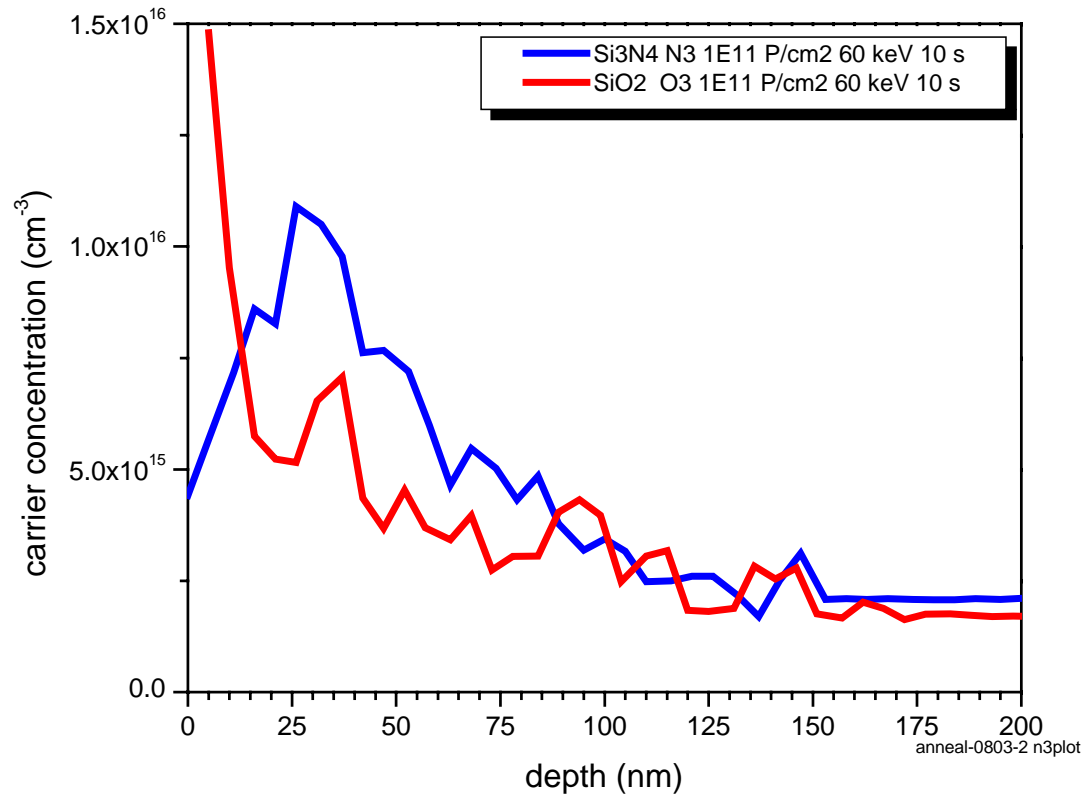
University of California, Lawrence Livermore National Laboratory, Livermore, California 94550



$T_{\text{ox}}=10\text{nm} \mid L_{\text{gate}}=1\mu\text{m} \mid N_{\text{sub}}: 3 \times 10^{11}\text{P} \mid$
S/D contours: $10^{14} \rightarrow 10^{20} \text{ P}$

- Medici simulation (2D) of charge pulse from single ion impact in a readout transistor channel at room temperature (C. C. Lo)

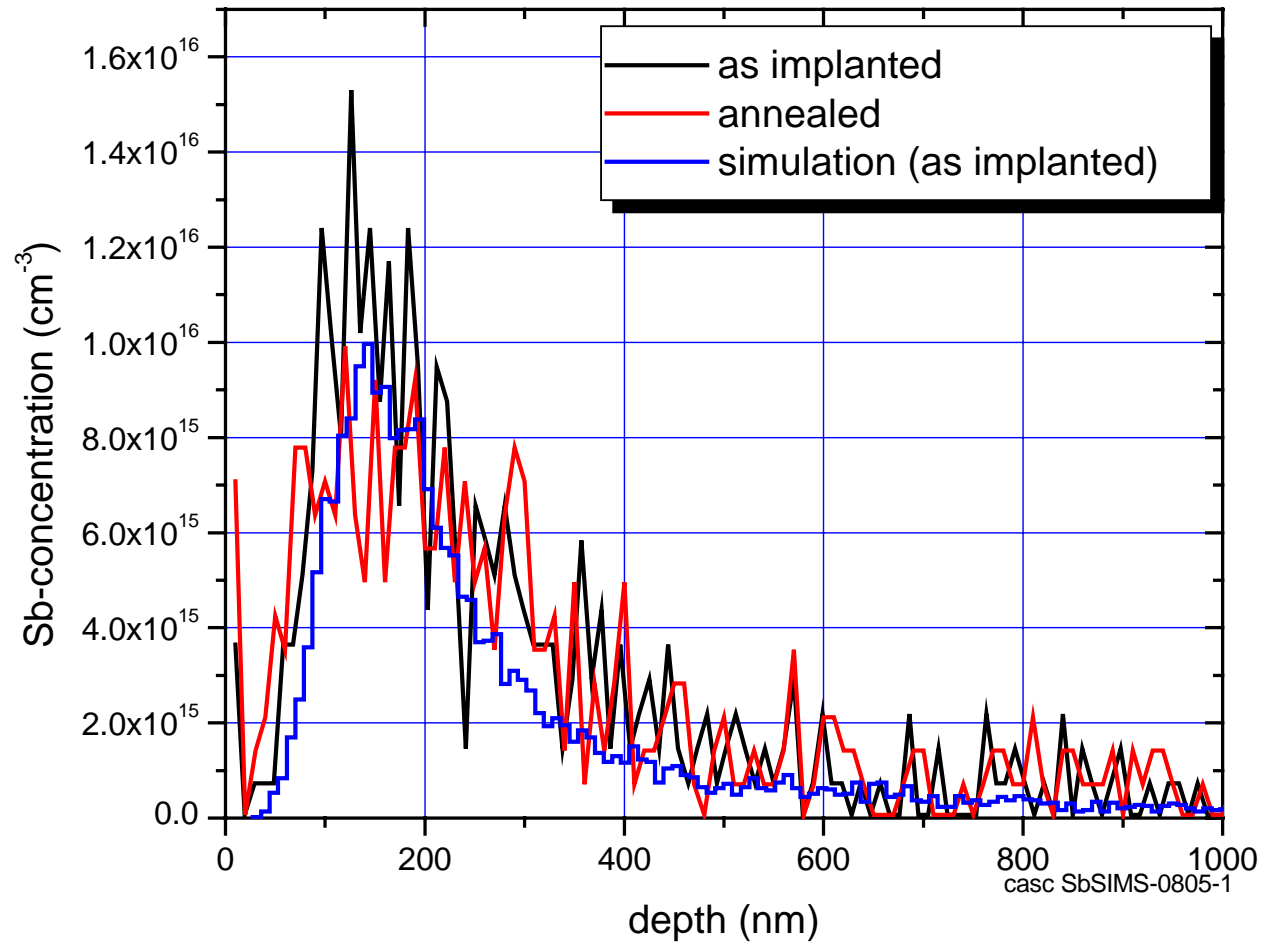
Interface effects on dopant diffusion / segregation



- injection of interstitials from the SiO₂/Si interface during annealing (or oxidation) drives ³¹P atoms to the interface, where dopants are not electrically active (and any array is completely dissolved)
- injection of vacancies from Si₃N₄/Si interface retards ³¹P segregation
- ¹²¹Sb shows the reverse effect, and is compatible with SiO₂/Si
- for theory see: J. Dabrowski, et al., Phys. Rev. B 65, 245305 (2002)

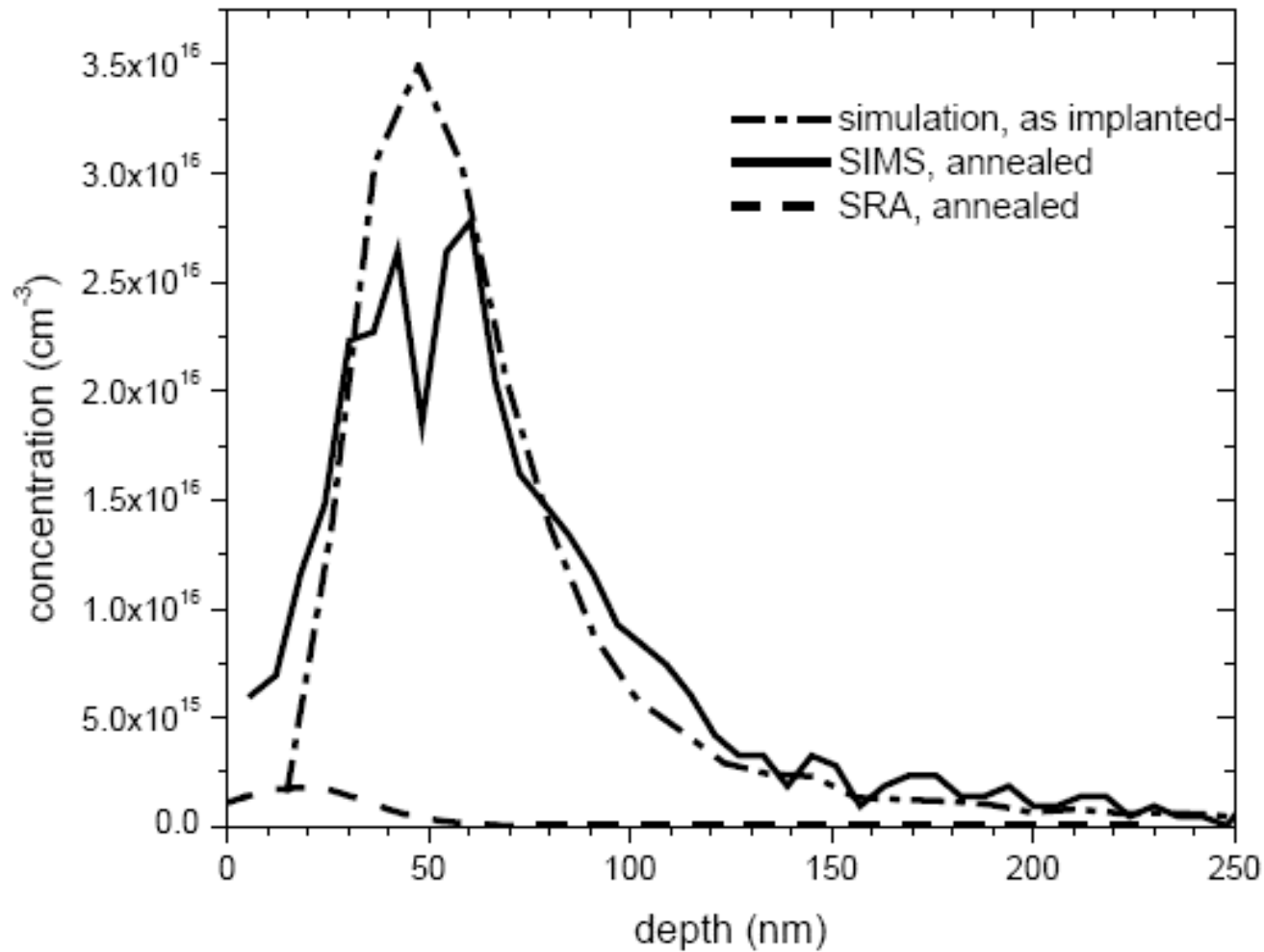
Improved Sb profile with annealing under oxidation conditions

– recent SIMS results



- 2E11 cm⁻², 121Sb, 400 keV, 1000 C, 10 s, O₂ anneal, Cs⁺ SIMS data by Cascade
- activation ~80%, SRA in progress

Antimony stays put !





Criteria for physical implementation of a quantum computer

(DiVincenzo)

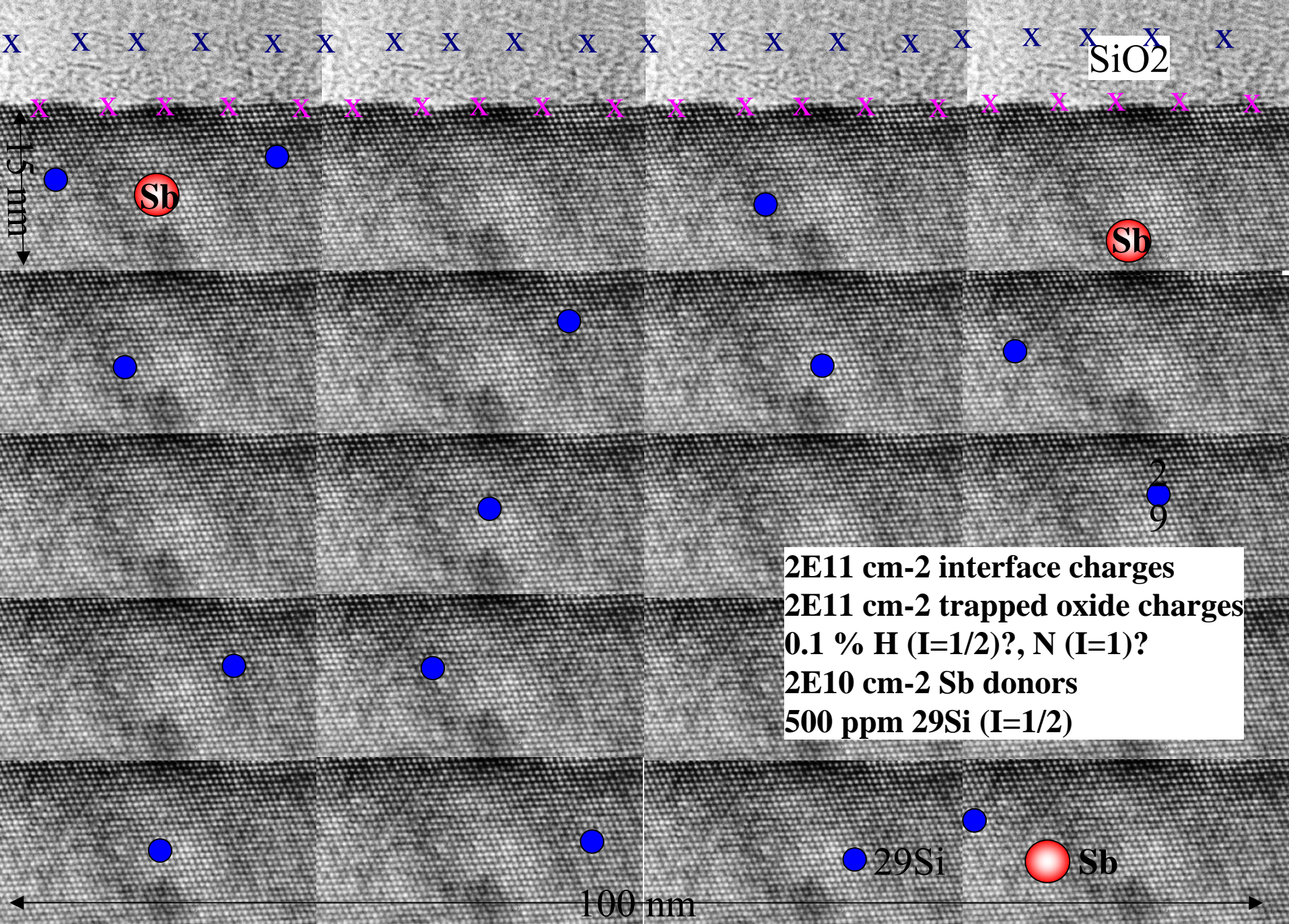
1. Well defined extendible qubit array – stable memory
 - Array of single donor atoms (P, As, Sb, Bi) in a silicon crystal matrix formed by single ion implantation (or STM-H lithography)
2. Initialization in the “000...” state
 - **polarization at low temperature, in strong magnet field, $kT \ll g\mu_B B$**
 - **kT (0.3 K) = 0.026 meV, $g\mu_B B$ (5 T) = 0.58 meV**
3. Long decoherence time ($>10^4$ operation time, to allow for error correction)
 - $T_2=T_1$ in pure ^{28}Si >10 s, limited by residual ^{29}Si , and by gate, and interface effects
4. Universal set of gate operations
 - Not: ESR rotations, need local B or g control
 - CNOT: two qubit interaction via J, or dipolar coupling, or RKKY, or e^- shuttling
5. Read-out (projective measurement)
 - Single shot, single spin readout, much faster than decoherence time
 - spin-to-charge conversion, spin dependent transport



Criteria for physical implementation of a quantum computer

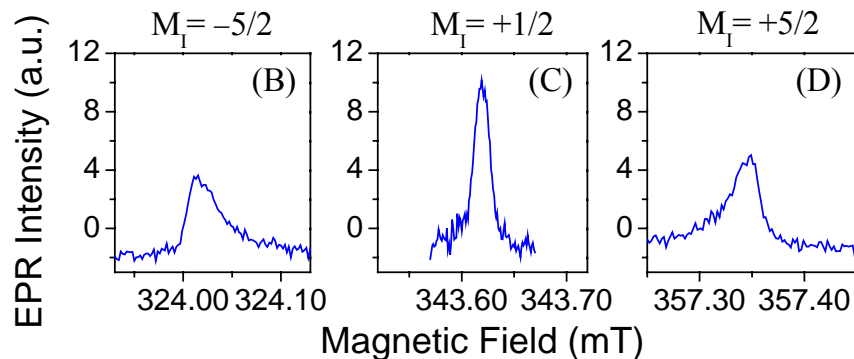
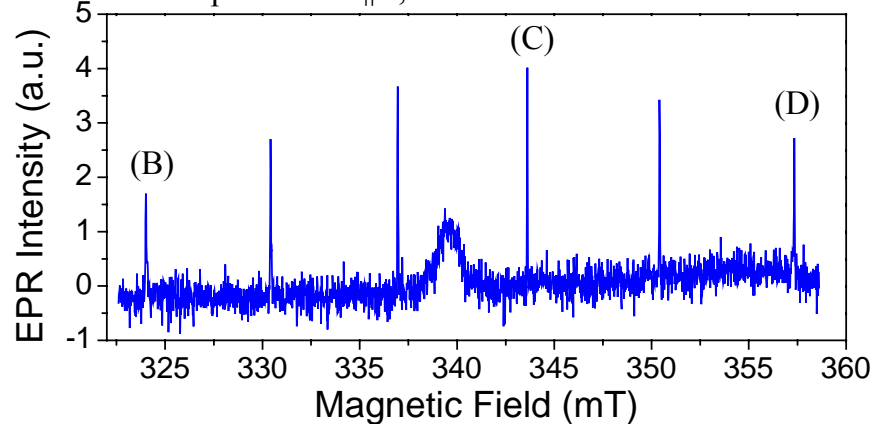
(DiVincenzo)

1. Well defined extendible qubit array – stable memory
 - Array of single donor atoms (P, As, Sb, Bi) in a silicon crystal matrix formed by single ion implantation (or STM-H lithography)
2. Initialization in the “000...” state
 - polarization at low temperature (0.3 K), in strong magnet field (5 T), $kT \ll g\mu_B B$
3. **Long decoherence time ($>10^4$ operation time, to allow for error correction)**
 - **$T_2 = T_1$ in pure $^{28}\text{Si} > 10$ s, limited by residual ^{29}Si , and by gate, and interface effects**
4. Universal set of gate operations
 - Not: ESR rotations, need local B or g control
 - CNOT: two qubit interaction via J, or dipolar coupling, or RKKY, or e^- shuttling
5. Read-out (projective measurement)
 - Single shot, single spin readout, much faster than decoherence time
 - spin-to-charge conversion, spin dependent transport



First ESR data on ^{121}Sb implanted ^{28}Si epi layers with thermal SiO_2 barriers (co. S. Lyon et al.)

Sample A ($\text{Sb}^{28}\text{Si } 2 \times 10^{10}$ anneal 60s at 1000C)
 Experiment: $n \parallel B$, $T = 6.2\text{K}$



in collaboration with Steve Lyon, Princeton
 \rightarrow use Sb due to P contamination in commercial ^{28}Si , at $5 \times 10^{13} \text{ cm}^{-3}$ level

- $T_2 = 0.3 \text{ ms}$ at 5 K ($T_1 = 10 \text{ ms}$), indication that electron spins are affected by coupling to the SiO_2/Si interface
- first step in optimization of pre-device structures by ensemble ESR

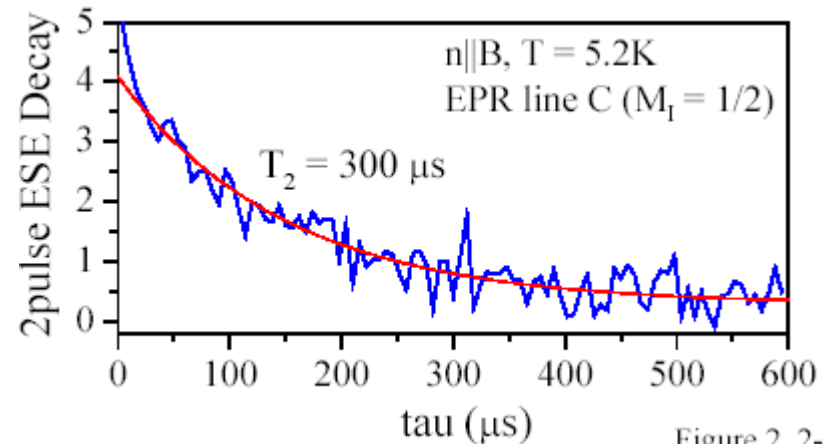
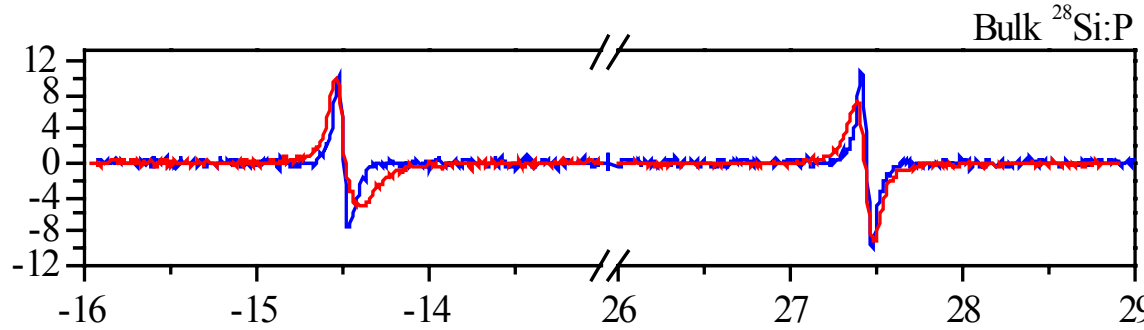
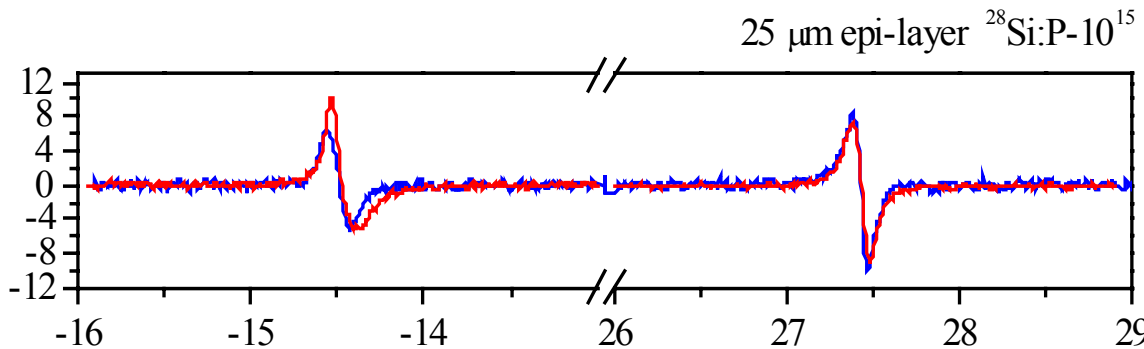


Figure 2.2.

Comparing implanted donors in pre-device to donors in “perfect” crystals: $T_2=0.3$ ms vs. 3 ms



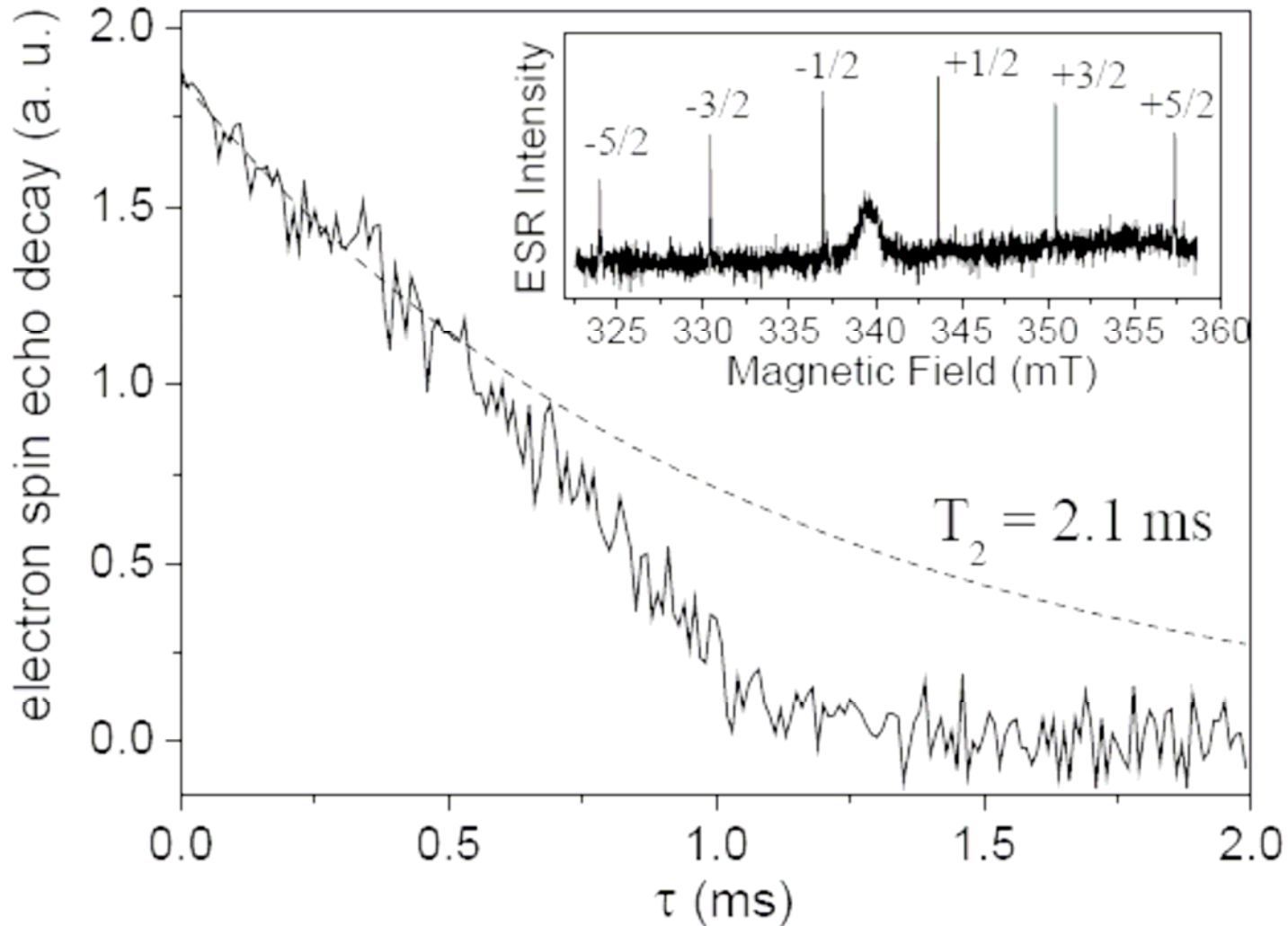
blue: ^{28}Si crystal,
 residual ^{31}P ($3\text{E}14 \text{ cm}^{-3}$)
 60 mG lines, $T_2 = 3$ ms
 red: ^{121}Sb implanted into ^{28}Si
 epi ($2\text{E}10 \text{ cm}^{-2}$, 120 KeV)



red: ^{28}Si epi layer,
 residual ^{31}P ($1\text{E}15\text{cm}^{-3}$)
 red: ^{121}Sb implanted into ^{28}Si
 epi ($2\text{E}10 \text{ cm}^{-2}$, 120 KeV)

^{31}P and ^{121}Sb have different hyperfine couplings (41.94 G and 66.7 G, respectively) and thus different hyperfine splitting in their EPR spectra. For comparison the magnetic field scale in the ^{121}Sb spectrum (red traces) was renormalized by factor 41.94/66.7. With this renormalization the degree of inhomogeneity in the ^{121}Sb spectrum can be directly compared to ^{31}P . It is seen that the ^{121}Sb lines show a larger lineshape difference than all the ^{31}P samples. However, T_2 is still 0.3 ms for the Sb, compared to 3 ms for the ^{28}Si crystal (with $3\text{E}14 \text{ cm}^{-3}$ P).

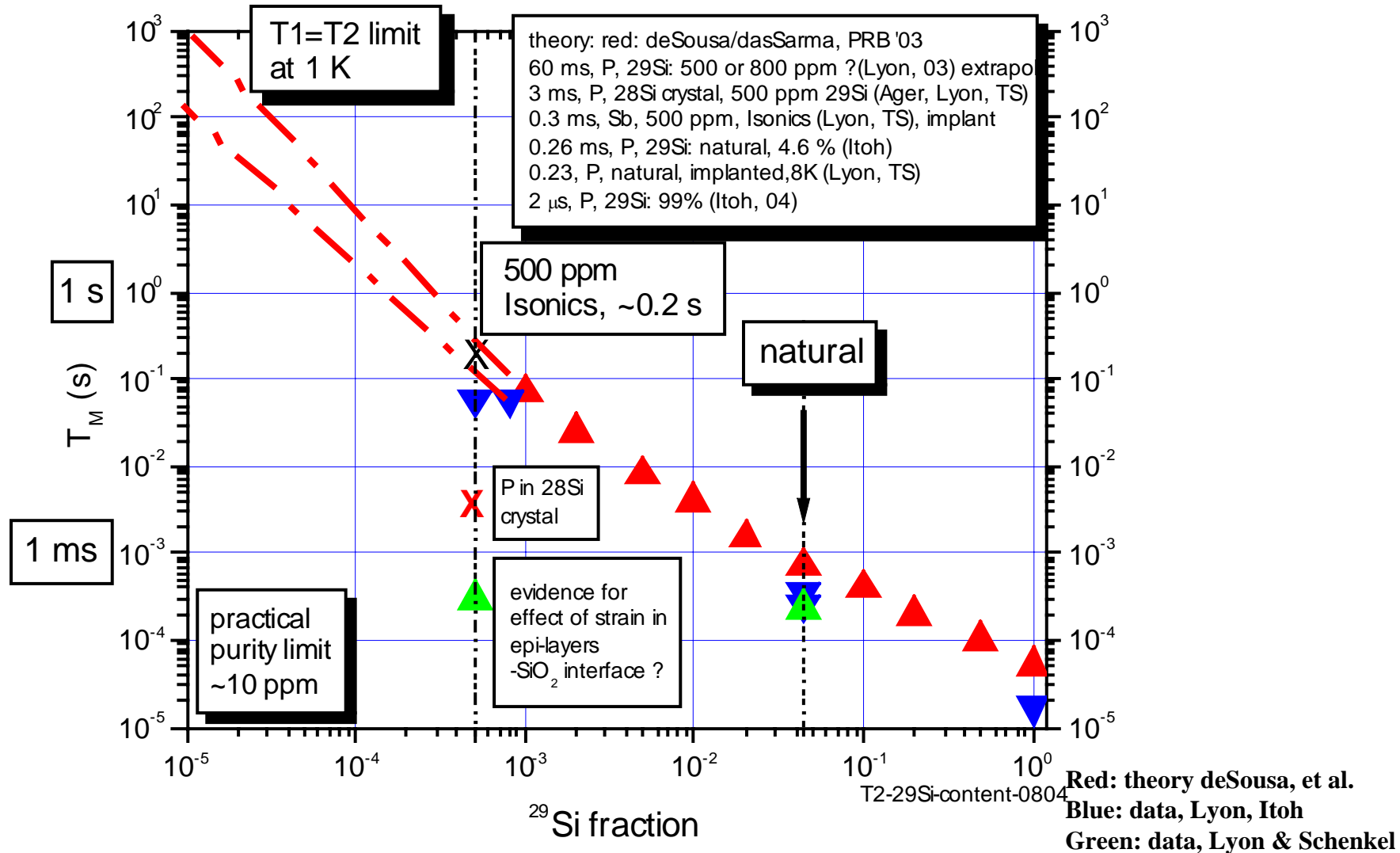
ESR: S. Lyon, and A. Tyryshkin



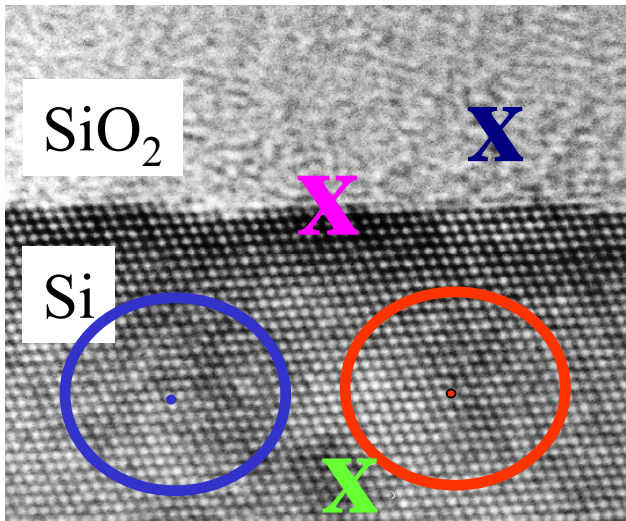
• instability of magnet limits coherence measurements >0.5 ms !

at 5 K

De-coherence times of donor electron spins in silicon: Limits due to ^{29}Si



T_2 increases when SiO_2 is removed and the silicon surface is passivated with hydrogen



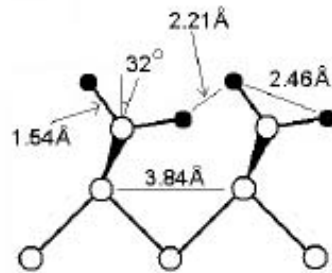
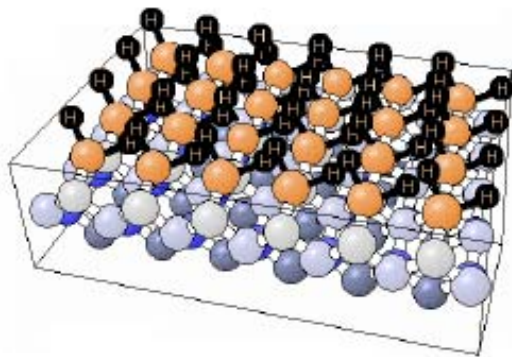
- expect temperature dependence of T_2 here since defect / trap dynamics is strongly temperature dependent ($1/f$ noise $\sim T^2$)

Interface	Average dopant depth (nm)	Activation ratio	T_1 (ms) at 5.2 K	T_2 (ms) at 5.2 K
Si_3N_4	20	0.1 %	-	-
SiO_2	20	0.8 %	10	0.3 +/-0.1
H-Si	20	-	-	0.75
SiO_2	60	70 %	10	1.5
H-Si	60	-	10	2.1

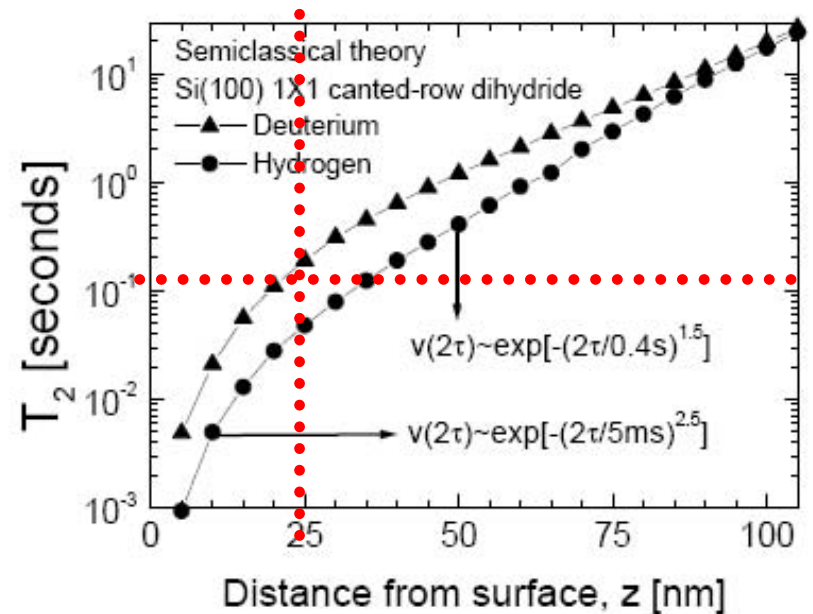
cond-mat/0507318
co. S. Lyon, R. deSousa, et al.

• ion implantation and standard CMOS processes are compatible with $T_2 \geq 1$ ms \rightarrow what is the T_2 limit in a device ?

Nuclear spin induced spectral diffusion limits T_2 for hydrogen terminated silicon surfaces – limit: $T_2 \approx 0.2$ s for d, and 25 nm deep donors (Rogerio De Sousa)



A Hydrogen terminated silicon surface is obtained after immersing the sample in a hydrogen fluoride solution. Here we show a Si(100)H surface with the hydrogen atoms forming a canted-row dihydride structure.¹⁵ The SiH₂ groups form a square lattice of side $5.43/\sqrt{2} = 3.84$ Å. Picture adapted from the NIST surface structure database and Ref. 15.



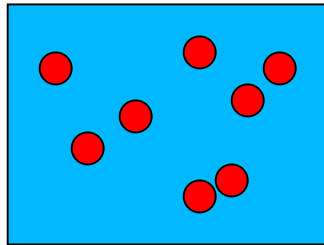
$1/e$ echo decay time (T_2) arising due to nuclear-induced spectral diffusion from hydrogen or deuterium nuclear spins in a Si(100)H surface as a function of donor depth. Circles hydrogen terminated surface, triangles deuterium.

- donor depth ~ donor spacing for top gate control
- nuclear spin effects also for $^{27}\text{Al}_2\text{O}_3$ ($I=5/2$), and $\text{Si}_3^{14}\text{N}_4$ ($I=1$)
- but no nuclear spin for (thermal) SiO_2 , where electronic defects can be less than one per device !
- ^{29}Si limit to T_2 at 500 ppm (commercial) is ~ 0.1 s (spectral diffusion theory, deSousa & DasSarma)

What limits coherence of donor electron spins in silicon ?

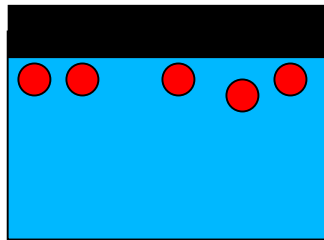
– from bulk to devices

S



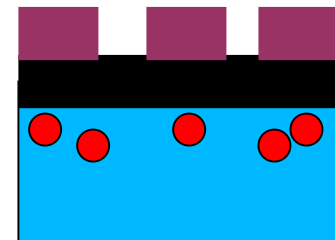
1. Randomly bulk doped natural silicon
Randomly bulk doped ^{28}Si crystals
Randomly bulk doped ^{28}Si epi layers

OS



2. Randomly ion implanted ^{28}Si epi layers with gate dielectrics (SiO_2 , Si_3N_4)

MOS



3. Randomly ion implanted ^{28}Si epi layers with gate dielectrics and gates

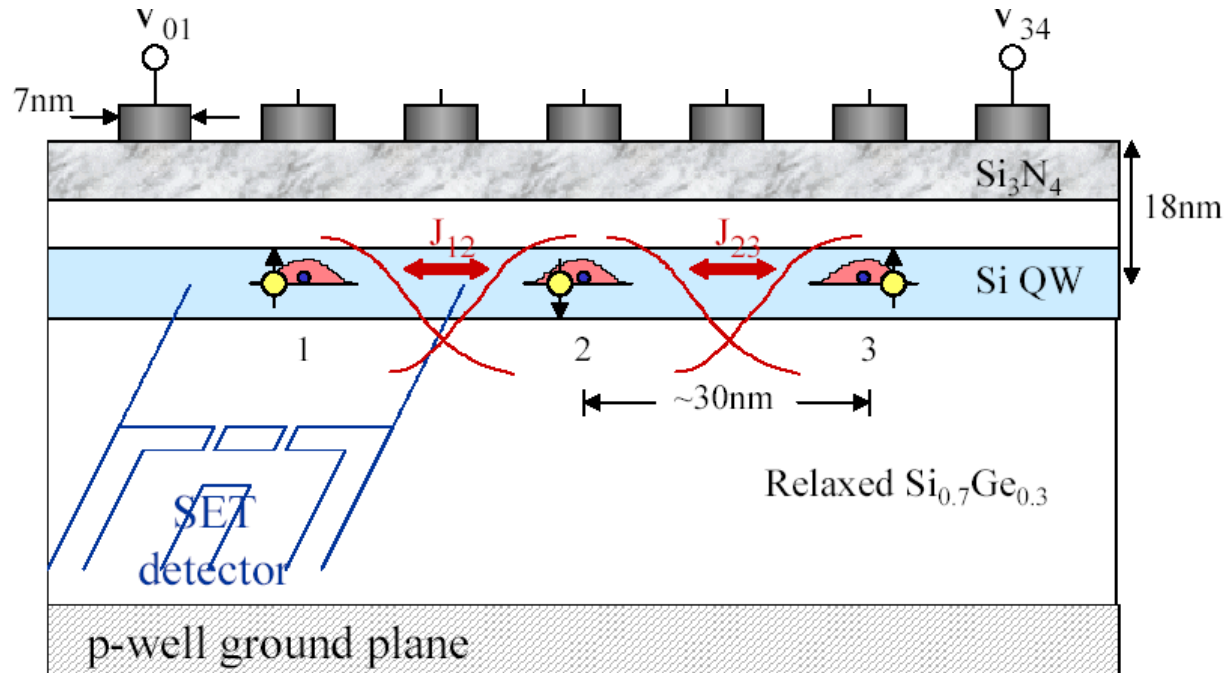
- Electron spin resonance (pulsed ESR) allows optimization of processes and materials in ensemble measurements with 10^{10} spins (S. Lyon, A. Tyryshkin, Princeton)
- optimize T_2 , understand coherence limiting factors, and use this to design and fabricate test devices



Criteria for physical implementation of a quantum computer

(DiVincenzo)

1. Well defined extendible qubit array – stable memory
 - Array of single donor atoms (P, As, Sb, Bi) in a silicon crystal matrix formed by single ion implantation (or STM-H lithography)
2. Initialization in the “000...” state
 - polarization at low temperature (0.3 K), in strong magnet field (5 T), $kT \ll g\mu_B B$
3. Long decoherence time ($>10^4$ operation time, to allow for error correction)
 - $T_2=T_1$ in pure ^{28}Si >10 s, limited by residual ^{29}Si , and by gate, and interface effects
4. **Universal set of gate operations**
 - **Not: ESR rotations, need local B or g control**
 - **CNOT: two qubit interaction via J, or dipolar coupling, or RKKY, or e⁻ shuttling**
5. Read-out (projective measurement)
 - Single shot, single spin readout, much faster than decoherence time
 - spin-to-charge conversion, spin dependent transport

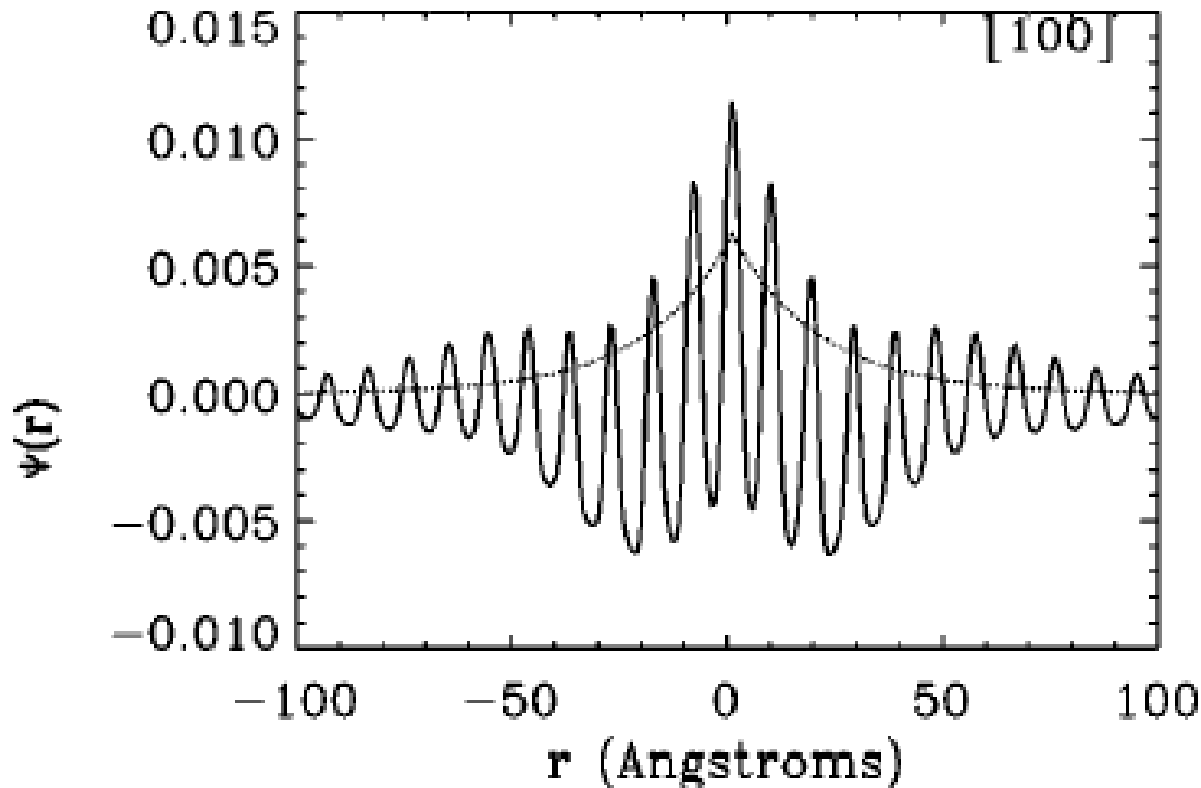


$$|0_L\rangle = |S\rangle|\uparrow\rangle$$

$$|1_L\rangle = (2/3)^{1/2}|T_+\rangle|\downarrow\rangle - (1/3)^{1/2}|T_0\rangle|\uparrow\rangle$$

- encoding of logical qubits in three electron spins allows universal QC with J only (DiVincenzo, Whaley '00), alleviating the need for single electron ESR, “just” pulsing gate electrodes

Degeneracy of Si conduction band edge leads to oscillations of donor wave functions and J coupling



The solid line shows Kohn-Luttinger wave function for a phosphorus donor electron in silicon, plotted along directions of high symmetry within the crystal. The dotted line shows an isotropic 1s hydrogenic wave function, with a Bohr radius of 20 Å.

C. J. Wellard et al., *Phys. Rev. B* 68, 195209 (2003)

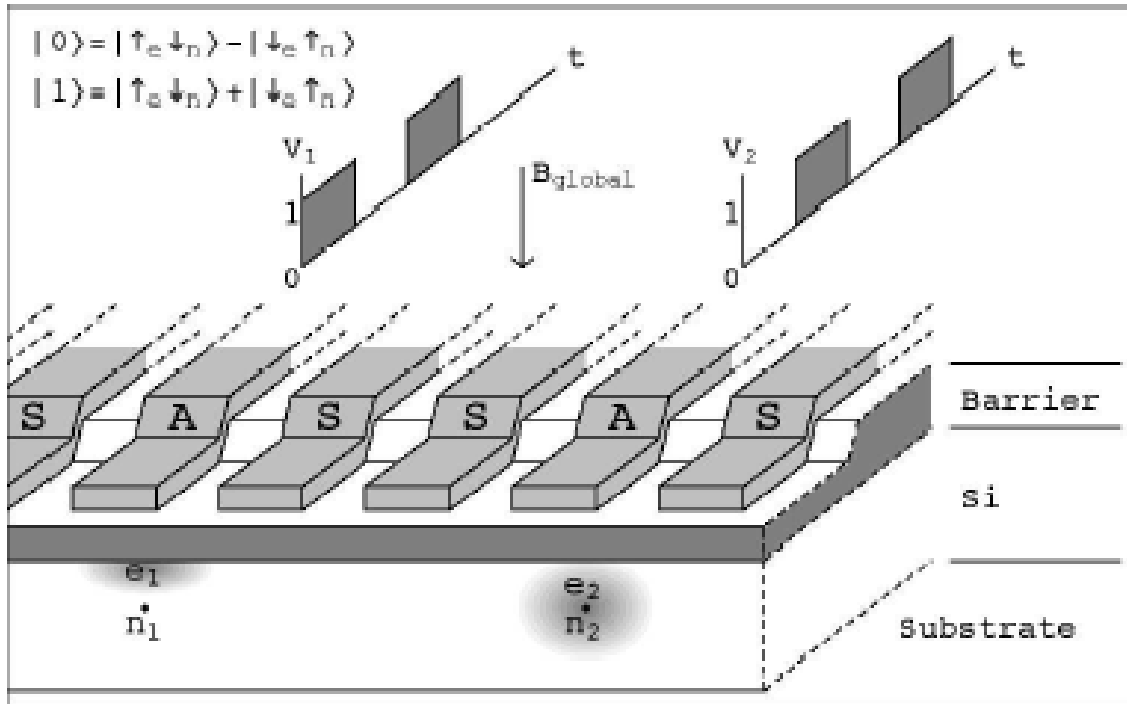
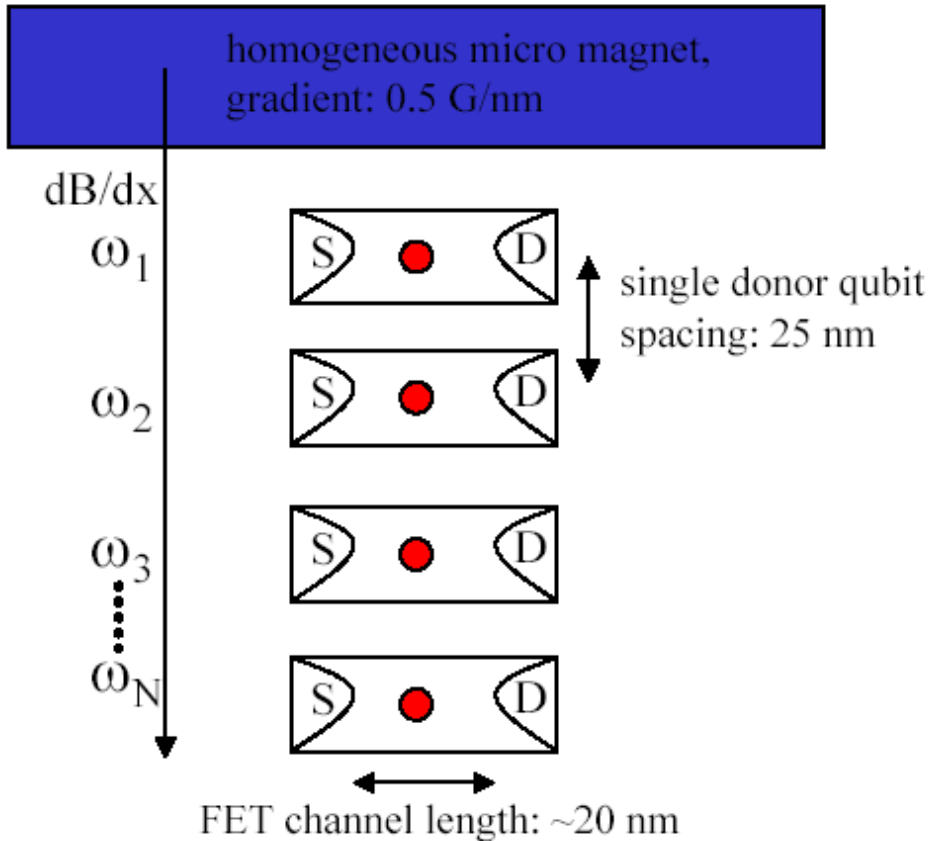


FIG. 1: Schematic of the proposed architecture. Each qubit is encoded in the spins of an electron and its donor nucleus. “A gates” above donor sites switch the electron-donor overlap, and thus the hyperfine interaction, while “S gates” shuttle electrons from donor to donor. “Bit trains” of voltages control the computer.

Skinner, Davenport, Kane '02
 Quant-ph/0206159

Donor electron spin qubit devices based on single spin rotations and dipolar coupling (co. Lyon, and deSousa)



Donor qubit Zeeman frequencies:

$$\omega_i = \gamma_i B_i$$

$$D_{12}(\theta, d) = \frac{\gamma_1 \gamma_2 \hbar}{d^3} (3 \cos^2 \theta - 1)$$

$$U_{\text{CZ}} = e^{-\frac{3\pi}{4}i} e^{\frac{3\pi}{2}iS_{1z}} e^{-\frac{\pi}{2}iS_{2z}} \exp\left(-i\frac{\pi}{D_{12}}\mathcal{H}_{12}\right)$$

- “always on” D can be tracked in 1 D arrays
- residual J treated as error with re-focusing protocols
- CNOT gate time ~ 0.1 ms, o. k. when T2 is optimized to > 1 s
- promising for demonstration of basic logic in devices with ~ 10 qubits

**R. deSousa et al.,
PRA 70, 052304 (2004)**

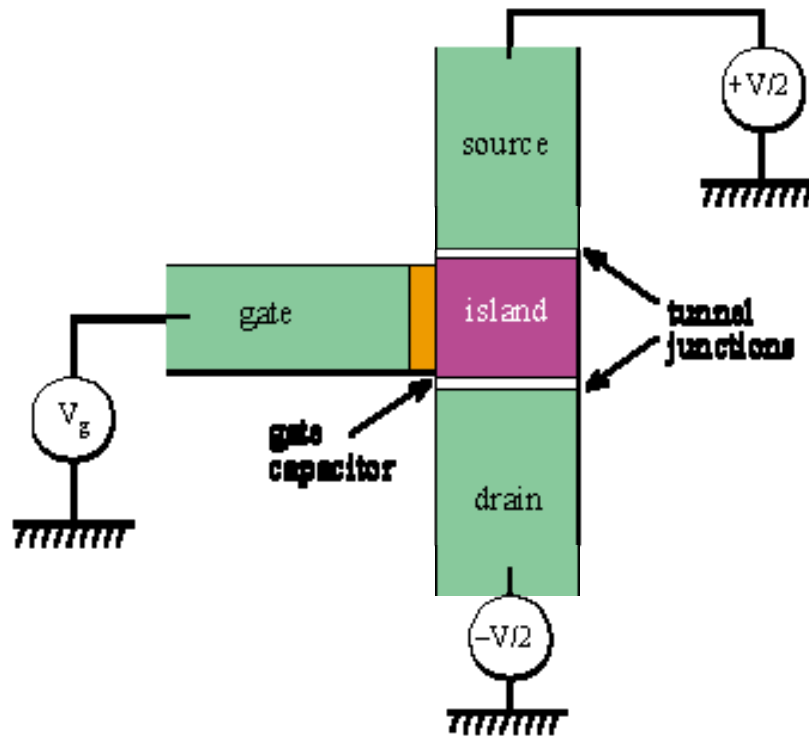


Criteria for physical implementation of a quantum computer

(DiVincenzo)

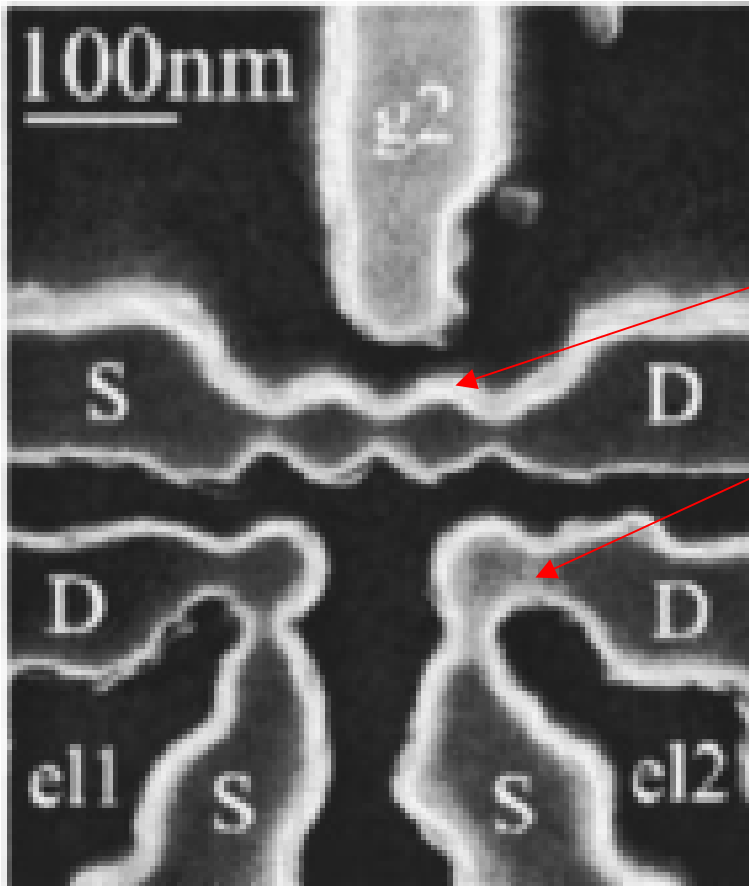
1. Well defined extendible qubit array – stable memory
 - Array of single donor atoms (P, As, Sb, Bi) in a silicon crystal matrix formed by single ion implantation (or STM-H lithography)
2. Initialization in the “000...” state
 - polarization at low temperature (0.3 K), in strong magnet field (5 T), $kT \ll g\mu_B B$
3. Long decoherence time ($>10^4$ operation time, to allow for error correction)
 - $T_2=T_1$ in pure ^{28}Si >10 s, limited by residual ^{29}Si , and by gate, and interface effects
4. Universal set of gate operations
 - Not: ESR rotations, need local B or g control
 - CNOT: two qubit interaction via J, or dipolar coupling, or RKKY, or e^- shuttling
5. **Read-out (projective measurement)**
 - **Single shot, single spin readout, much faster than decoherence time**
 - **spin-to-charge conversion, spin dependent transport**

Single electron transistor as a sensitive electrometer



- charging energy for electrons to hop onto island: $E_c = e^2/2C \gg kT$
- tunneling “resistance” $R \gg 1/G = h/e^2 = 26 \text{ k}\Omega$
- need $E_c \sim 10 \text{ kT}$ for reliable operation
- LHe, 4 K, $kT = 0.34 \text{ meV}$
- SET at room temperature: capacitance of island $\sim 1 \text{ aF}$, size smaller than 10 nm

SET as a sensitive electrometer



SiGe double dot structure

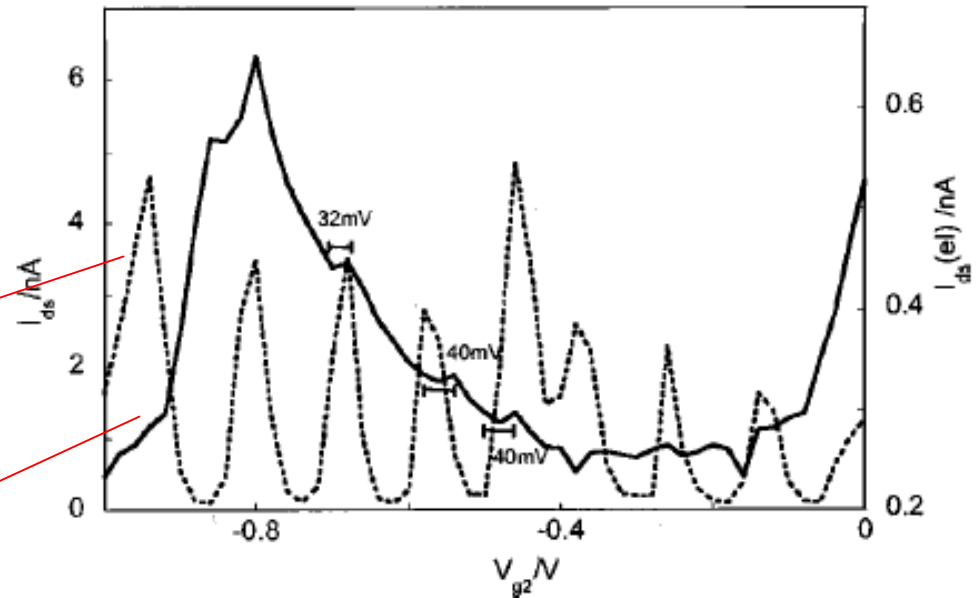
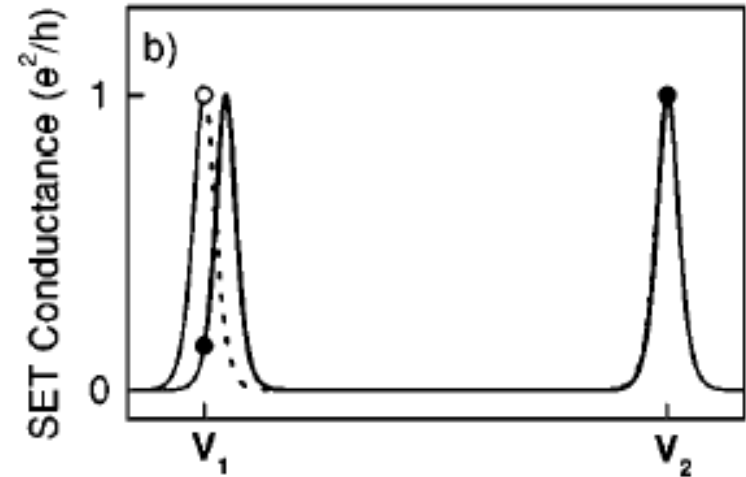
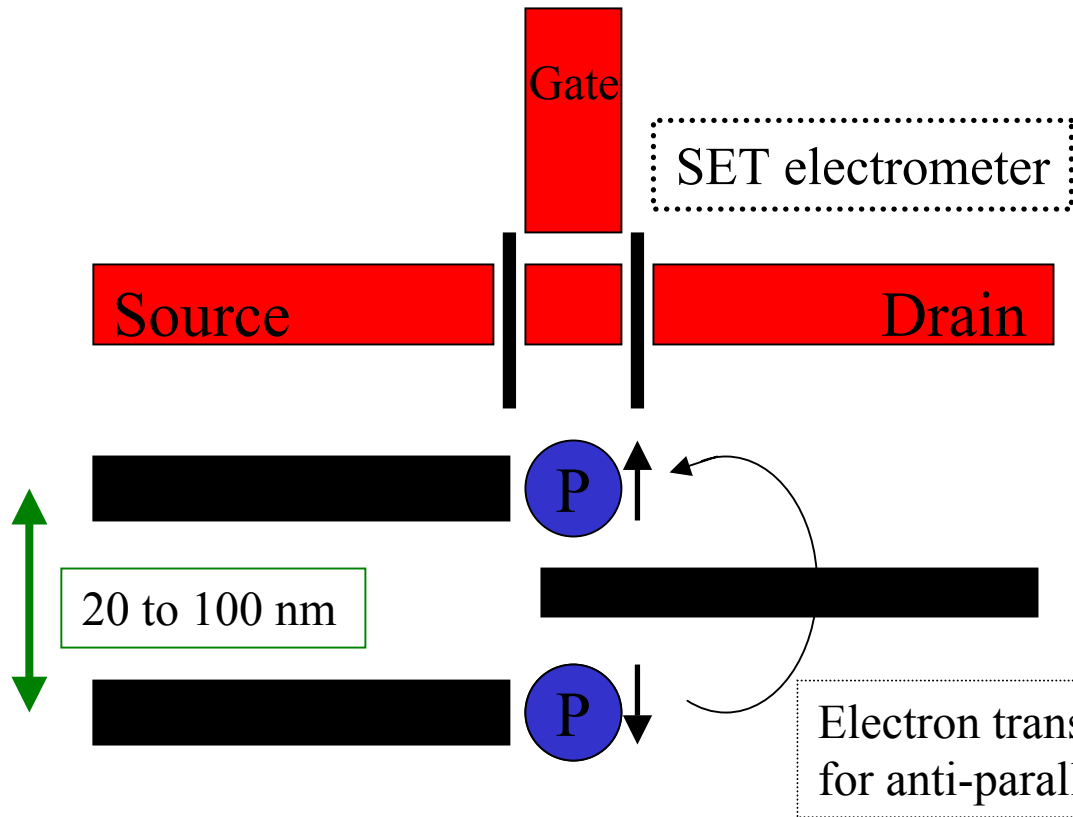


FIG. 9. Coulomb oscillations measured simultaneously in the electrometer e12 (solid) and the central dot structure (dotted), using gate g_2 . Every time the hole number on the central dot structure changes by one (by passing through a Coulomb oscillation) a kink is seen in the Coulomb oscillations of e12.

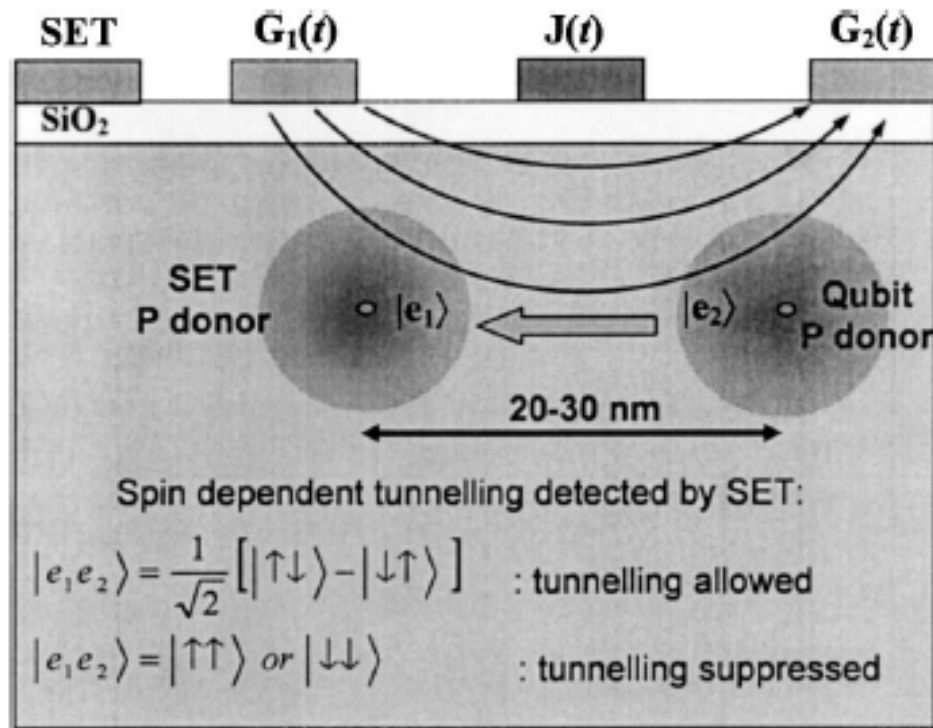
From: Cain et al, JAP 92, 346 (2002)

Basic building block to access the physics of the ^{31}P qubit: Two ^{31}P atoms aligned with control gates and SETs



Kane et al., PR B 61, 2961 (2000)

- Gate control of single spins and read out through spin dependent charge transfer between ^{31}P atoms (based on singlet-triplet splitting and exclusion principle)
- For two spins there are three symmetric (triplet) states: $\uparrow\uparrow, \uparrow\downarrow + \downarrow\uparrow, \downarrow\downarrow$ and one anti-symmetric (singlet) state: $\uparrow\downarrow - \downarrow\uparrow$



Spin readout
via D⁻ and SET

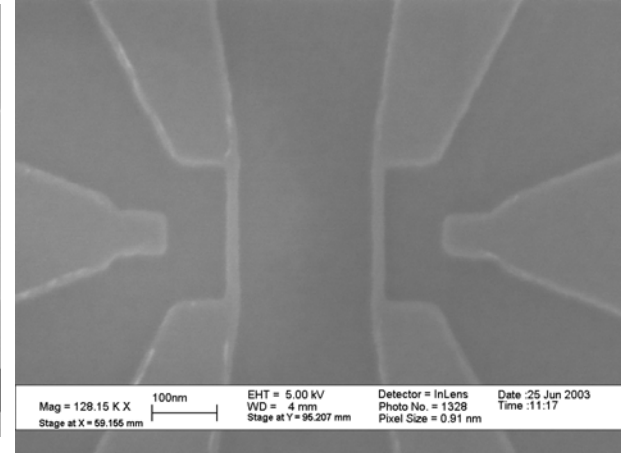
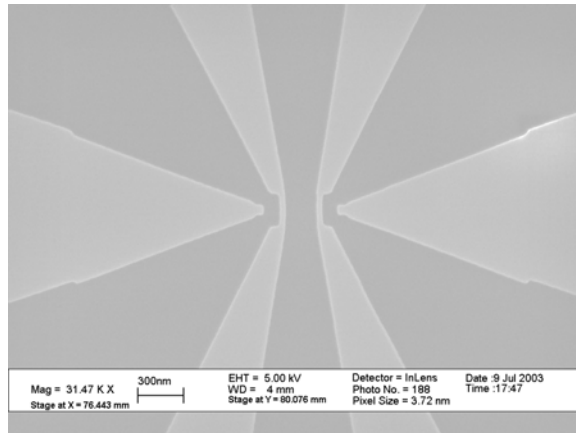
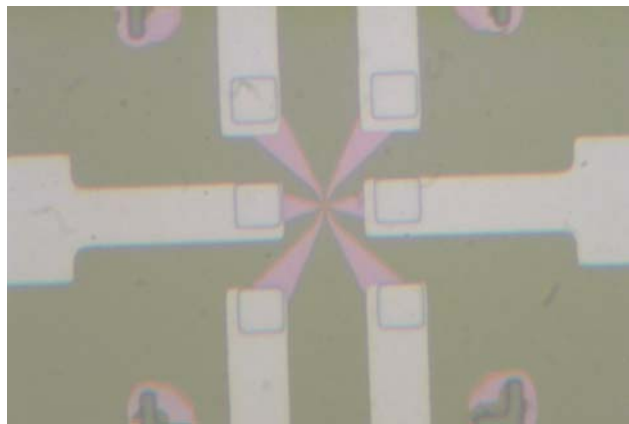
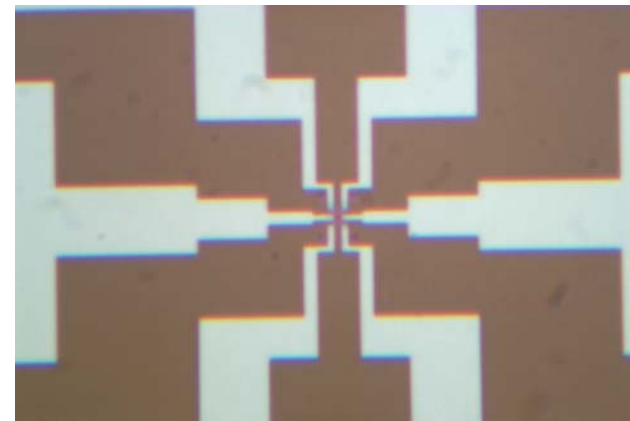
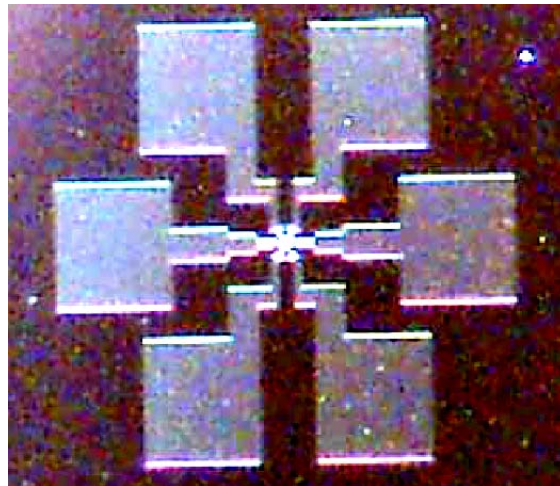
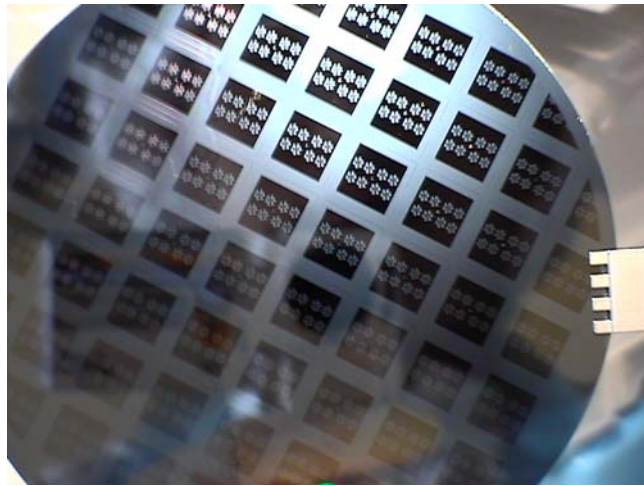
Hollenberg, et co.,
-PRB 69, 233301 (2004)
-cond-mat/0403449

FIG. 1. Spin-dependent charge transfer scheme for single-spin readout based on dopant atoms in semiconductors.

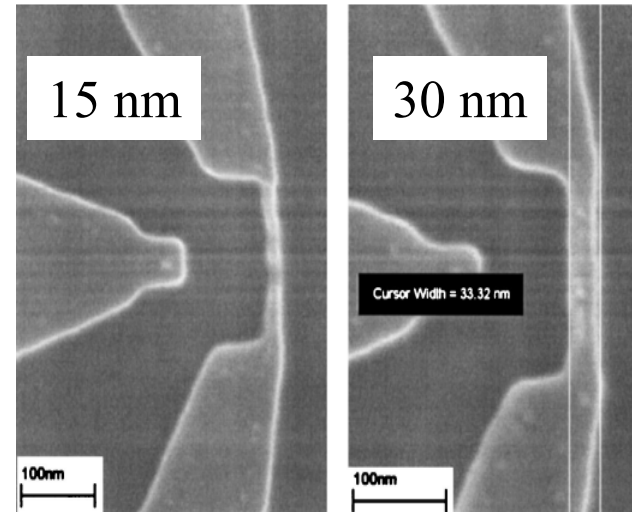
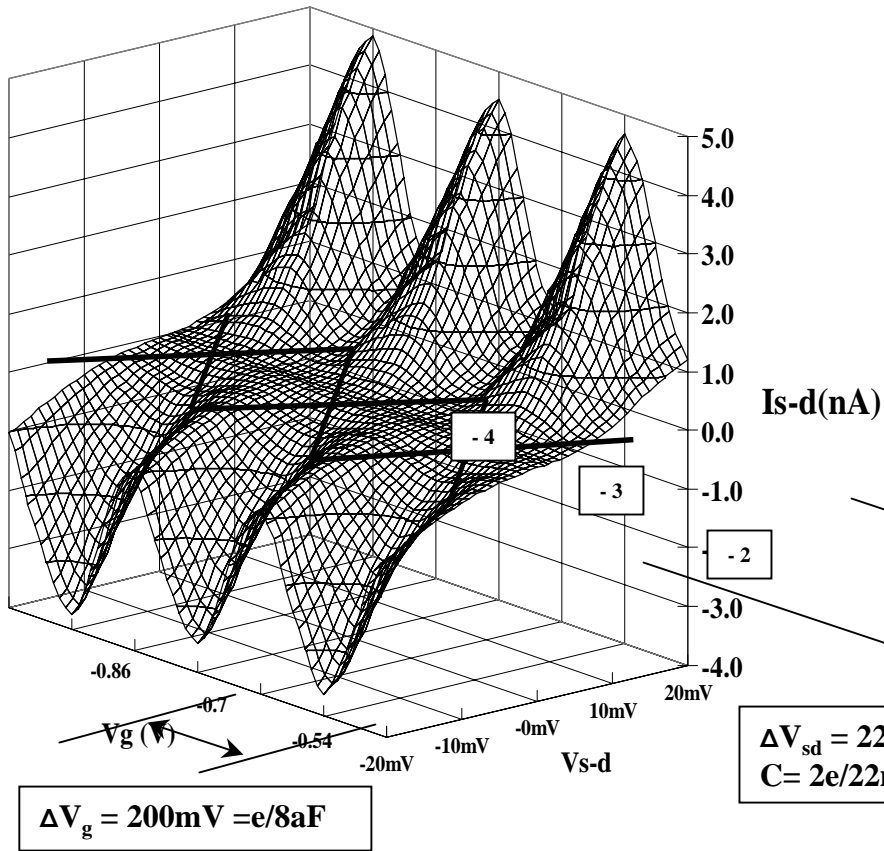
with a single electron transistor (SET) [9]. Although the D⁺D⁻ state has been observed via far-infrared transmission [10], under the conditions required to adiabatically form the D⁺D⁻ system in a top-gate controlled structure, it appears that the state will be quasi-bound, with a lifetime incompatible with SET readout [9].

- single shut SET measurement time vs. adiabatic gating to avoid D⁻ ionization

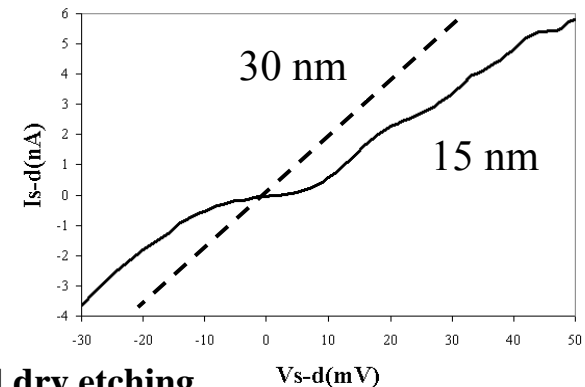
Si-SETs in SOI with 10 nm line widths



Silicon nanowire SETs - direct lithographic access to 15 nm wires in SOI without stress limited oxidation



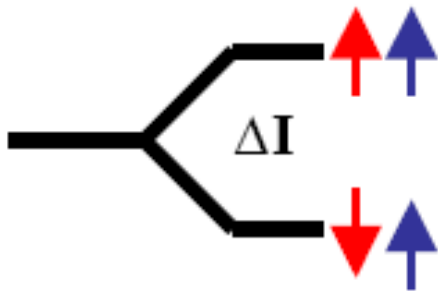
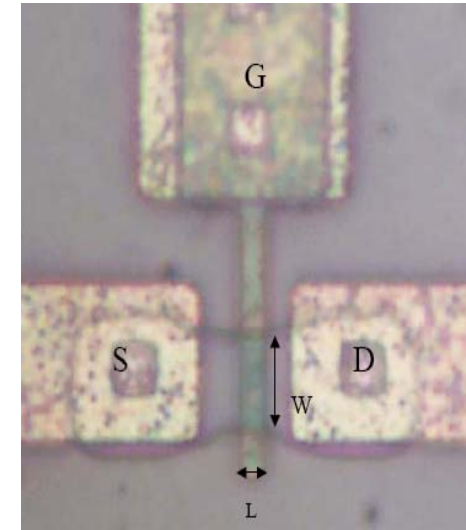
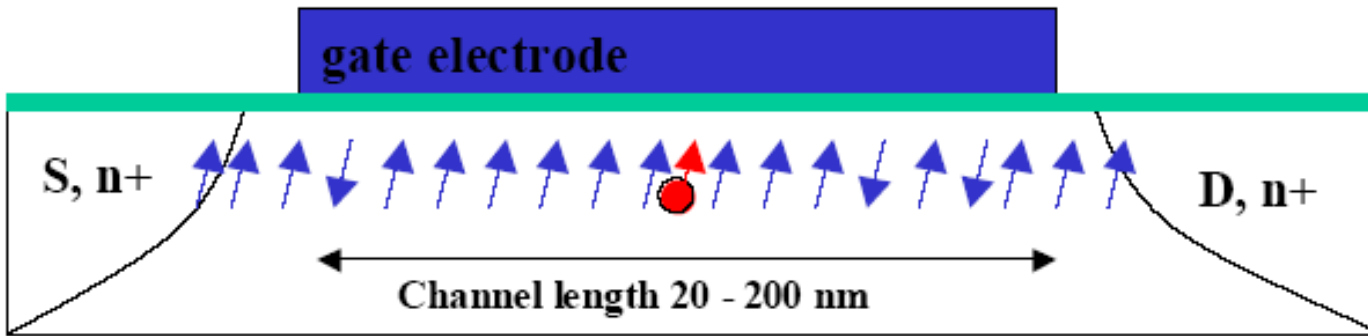
$\Delta V_{sd} = 22\text{mV}$
 $C = 2e/22\text{mV} = 15\text{aF}$



- direct lithographic control at 10 nm level in Silicon by e-beam lithography and dry etching
- SET islands and tunnel junctions form by dopant segregation during source-drain implant anneals
- **issue: electronic defects at SiO₂/Si interface will affect decoherence of nearby donor spins**

S. J. Park et al., J. Vac. Sci. Technol. B 22, 3115 ('04)

Single Spin Readout via Spin Dependent Transport in FET channel



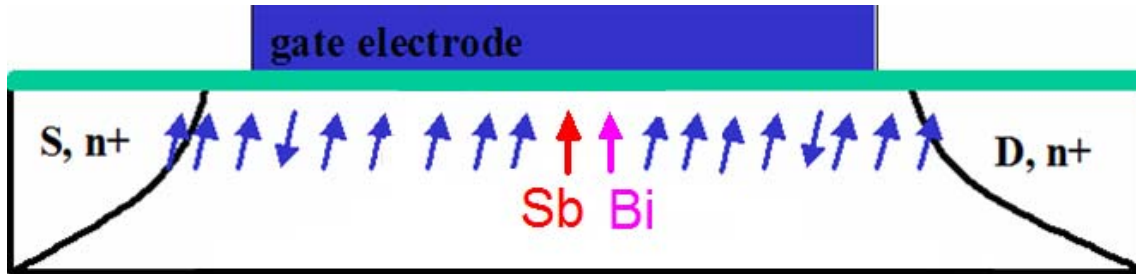
$$\frac{\Delta I_{\uparrow\uparrow}}{I_0} \approx \text{const.} \times \sigma_{\text{tri}}$$

$$\frac{\Delta I_{\downarrow\uparrow}}{I_0} \approx \text{const.} \times \left(\frac{\sigma_{\text{tri}} + \sigma_{\text{si}}}{2} \right)$$

$$\sigma_{\text{si}} - \sigma_{\text{tri}} \geq 4 \times 10^{-13} \text{ cm}^{-2}$$

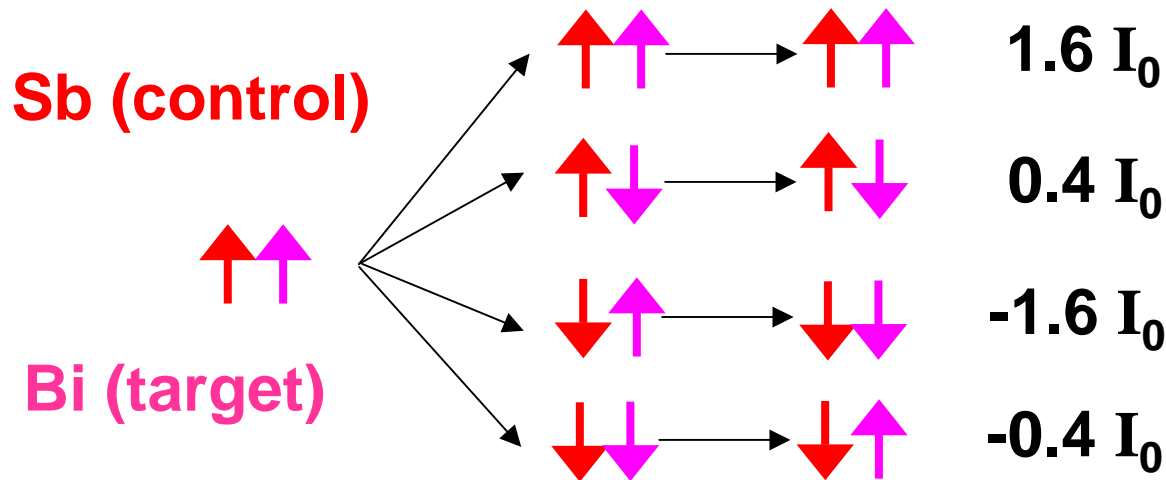
- injected spins will be slightly polarised (at least a few percent), donor spins will be up or down
- for in-up – donor-up: only triplets can form, for in-up – donor-down: singlets and triplets form with 50% probability
- neutral impurity scattering has to be comparable to other scattering mechanisms (mostly from interface roughness)
- demonstrated for 10^8 spins in mm scale transistors by Ghosh, and Silsbee, PRB 46, 12508 (1992)
- effect of $dI/I_0 \sim 10^{-4}$ for $\sim 1000 \text{ nm}^2$ per dopant atom, enhanced for smoother interfaces (H-Si, better SiO_2 , ...)
- **this effect is sensitive to the donor species due to different Bohr radii, 1.85 nm (Sb) vs. 1.45 nm (Bi) $\rightarrow \sigma_{\text{Sb}}/\sigma_{\text{Bi}}=1.6$**
- readout time is limited by spin flip time when transistor is on (off state T_1 , $\sim 10^3$, will determine on state T_1)

Proof of principle experiment: Demonstrate CNOT for a Sb-Bi pair in one readout channel (co. R. De Sousa)

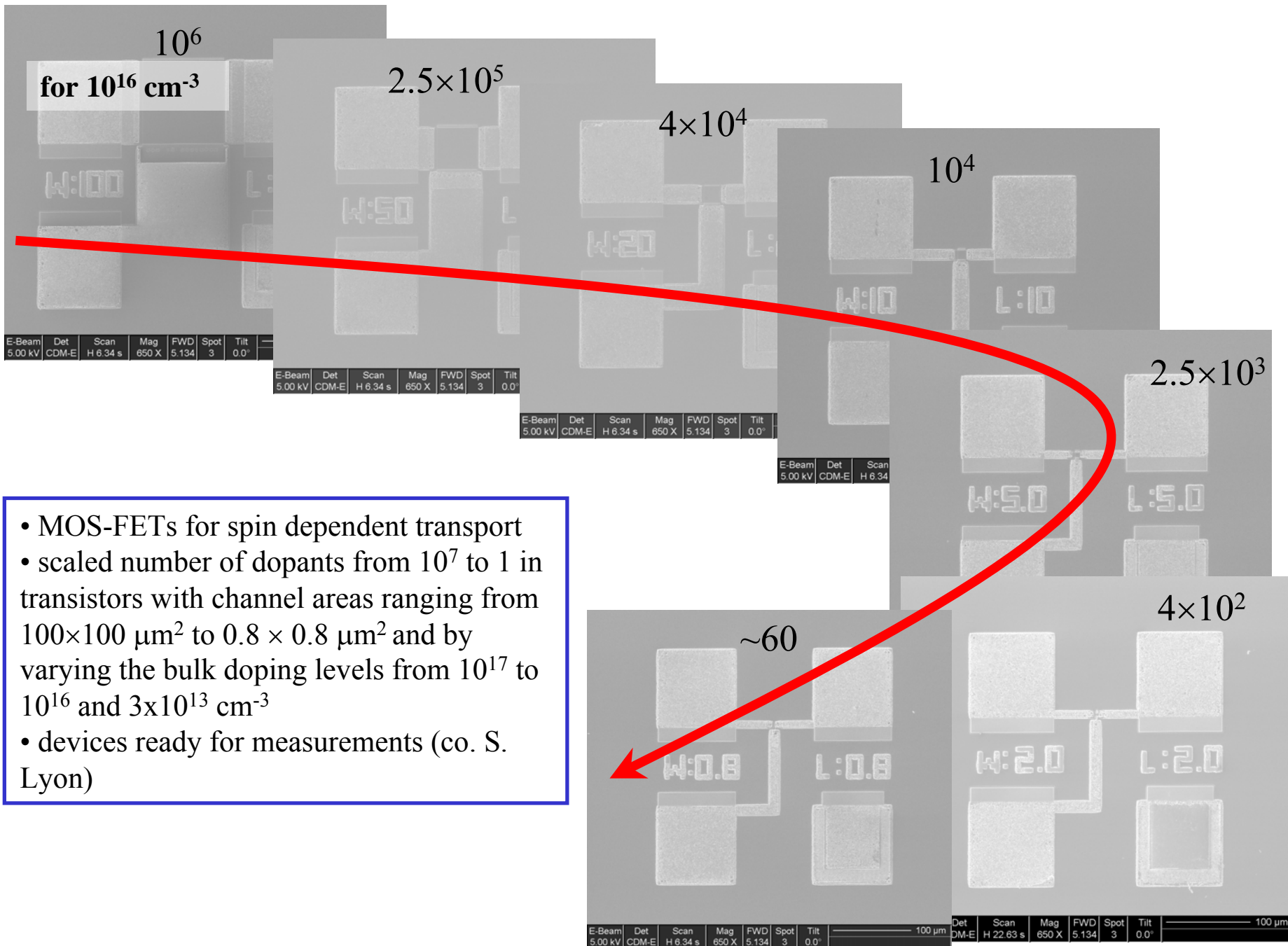


$$U_{CNOT} = e^{-i\frac{\pi}{2}S_{2y}} e^{-i\frac{\pi}{2}S_{2z}} e^{i\pi S_{1z}S_{2z}} e^{i\frac{3\pi}{2}S_{1z}} e^{i\frac{\pi}{2}S_{2y}}$$

Preparation Evolution Detection



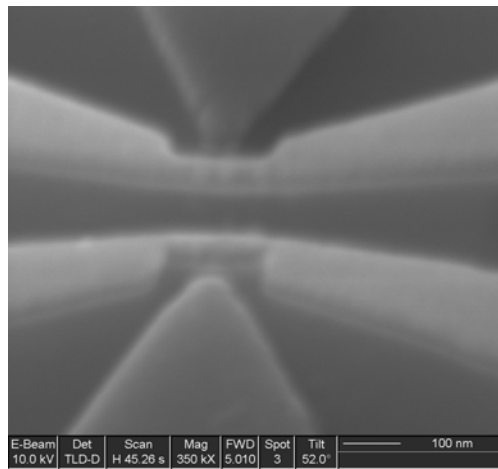
- once that's done: extension to qubit arrays & networks
- (if there is anything we know how to integrate and scale, it's transistors...)



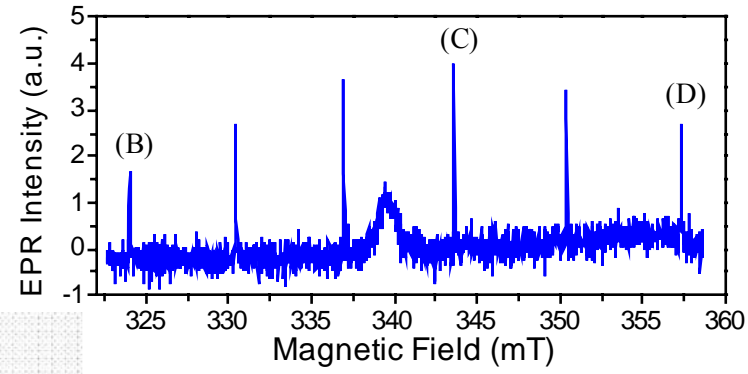
- MOS-FETs for spin dependent transport
- scaled number of dopants from 10^7 to 1 in transistors with channel areas ranging from $100 \times 100 \mu\text{m}^2$ to $0.8 \times 0.8 \mu\text{m}^2$ and by varying the bulk doping levels from 10^{17} to 10^{16} and $3 \times 10^{13} \text{ cm}^{-3}$
- devices ready for measurements (co. S. Lyon)

Spin qubits have potential for large scale quantum computation (but we are still at the stage of rudimentary demonstrations)

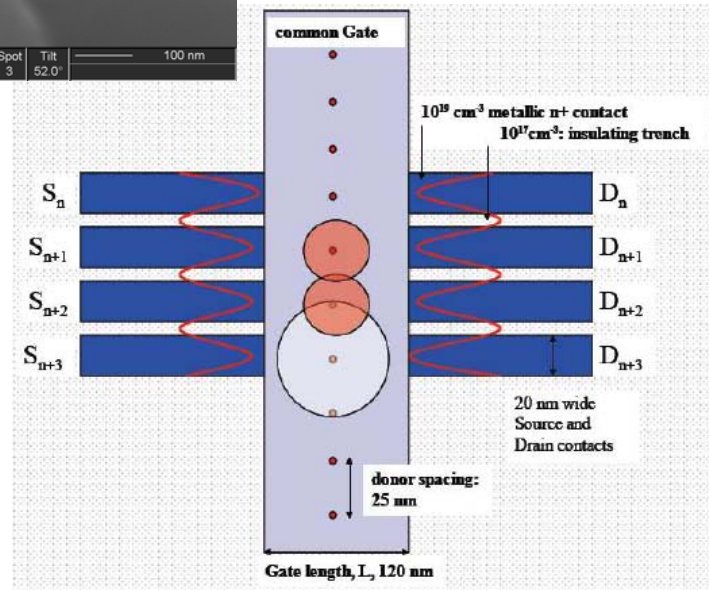
well tempered silicon transistors



microwave control of donor electron spins

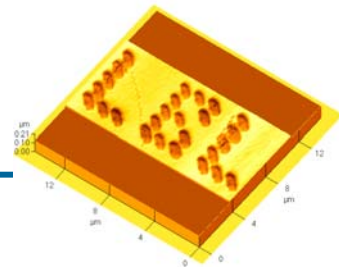


=



Path to large scale quantum computation
(>10,000 qubits)

Acknowledgments



- **Graduate students**

- Arun Persaud
- Sang-Joon Park
- Francis Allen
- Cheuk Chi Lo

- **Undergrad. Student**

- Jason Shangkuan

- **Special thanks to**

- Staff of the UC Berkeley Microlab
- Staff of the LBNL-NCM for TEM and FIB support

- **Contact:**

- T_Schenkel@LBL.gov
- <http://www-ebit.lbl.gov/>

- **Team members and collaborators**

- Jeff Bokor, UC Berkeley & LBNL
- Sunghoon Kwon, Molecular Foundry, LBNL
- Alex Liddle, LBNL
- Ivo Rangelow, Kassel University
- Ivan Chakarov, Silvaco, Santa Clara, CA
- Dieter Schneider, LLNL
- T-C Shen, Utah State University
- John R. Tucker, University of Illinois
- Joel Ager, LBNL
- Steven Lyon, Princeton University
- Alexei Tyryshkin, Princeton University
- Rogerio deSousa, UC Berkeley
- Birgitta Whaley, UC Berkeley



This work is supported by NSA and NSF

